

Universiteit
Leiden
The Netherlands

Role of TNF-α and the NF-κB pathway in drug-induced organ injuries

Benedetti, G.O.E.

Citation
Benedetti, G. O. E. (2013, May 7). *Role of TNF-α and the NF-κB pathway in drug-induced organ injuries*. Retrieved from https://hdl.handle.net/1887/20857

Version:	Corrected Publisher's Version
License:	Licence agreement concerning inclusion of doctoral thesis in the Institutional Repository of the University of Leiden
Downloaded from:	https://hdl.handle.net/1887/20857

Note: To cite this publication please use the final published version (if applicable).

Cover Page



Universiteit Leiden



The handle http://hdl.handle.net/1887/20857 holds various files of this Leiden University dissertation.

Author: Benedetti, Giulia
Title: Role of TNF-α and the NF-κB pathway in drug-induced organ injuries
Issue Date: 2013-05-07



5



The NF–κB family member RelB facilitates apoptosis of renal epithelial cells caused by cisplatin/TNF–α synergy by suppressing an EMT–like phenotypic switch

Giulia Benedetti[1], Michiel Fokkelman[1], Kuan Yan[2], Lisa Fredriksson[1], Bram Herpers[1], John Meerman[1], Bob van de Water[1] and Marjo de Graauw[1]

[1] Division of Toxicology, Leiden/Amsterdam Center for Drug Research, Leiden University, The Netherlands

[2] Section Imaging and Bioinformatics, Leiden Institute of Advanced Computer Science, Leiden University, The Netherlands

Conditionally accepted pending revision at Molecular Pharmacology

Abstract

Cisplatin-induced renal proximal tubular apoptosis is known to be preceded by actin cytoskeleton reorganization, in conjunction with disruption of cell-matrix and cell-cell adhesion. In the present study we show that the pro-inflammatory cytokine tumor necrosis factor α (TNF-α) aggravated these cisplatin-induced F-actin and cell adhesion changes, which was associated with enhanced cisplatin-induced apoptosis of immortalized proximal tubular epithelial cells (IM-PTECs). TNF-α induced RelB expression, and lenti-viral shRNA-mediated knock-down of RelB, but not other NF-κB members, abrogated the synergistic apoptosis observed with cisplatin/TNF-α treatment to the level of cisplatin-induced apoptosis. This protective effect was associated with increased stress fibre formation, cell-matrix and cell-cell adhesion in the shRelB cells during cisplatin/TNF-α treatment, mimicking an epithelial-to-mesenchymal phenotypic switch. Indeed, gene array analysis revealed that knock-down of RelB was associated with up-regulation of several actin regulatory genes, including snail2 and the Rho GTPase proteins Rhophilin and ARHGEF3. Pharmacological inhibition of Rho kinase signalling, re-established the synergistic apoptosis induced by combined cisplatin/TNF-α treatment of shRelB cells. In conclusion, our study shows for the first time that RelB is required for the cisplatin/TNF-α-induced cytoskeletal reorganization and apoptosis in renal cells by controlling a Rho kinase-dependent signalling network.

1. Introduction

Acute renal failure (ARF) refers to a sudden deterioration of kidney function and is caused by either ischemia/reperfusion (I/R) or exposure to nephrotoxic xenobiotics like cisplatin (1). The proximal tubular epithelial cells (PTECs) are the primary target. After ischemic or nephrotoxic injury, morphological alterations occur in these PTECs. Disruption of the actin cytoskeleton of the PTECs is an early event, leading to loss of adhesion of cells from the extracellular matrix (ECM) as well as neighbouring cells, ultimately resulting in loss of cell function, pro-apoptotic signalling and cell death (2-8). Given the central role of the actin cytoskeletal network in cell adhesion maintenance and PTEC injury, it is important to better understand the molecular signalling networks that regulate the F-actin cytoskeleton organization in PTECs and, thereby, cell adhesion and cell survival during renal cell injury stress responses.

The actin cytoskeleton reorganization that takes place prior to and during PTEC injury, is directly associated with changes in cell-matrix and cell-cell adhesion. We

have previously shown that exposure to nephrotoxic compounds, including cisplatin, affects the actin cytoskeleton network accompanied by disruption of focal adhesions (FA) followed by subsequent cell detachment and cell death in renal epithelial cells (6, 7, 9-11). In addition, cisplatin treatment induces a loss of the tight junction and adherens junction proteins β-catenin and zona-occludens 1 (ZO-1) at the cell membrane in mouse proximal tubular cells and preservation of the cell-cell junctions protects against cisplatin-induced apoptosis (12, 13). Understanding which PTEC signalling programs can control the actin signalling network, may lead to new therapeutic avenues to protect against cell detachment and cell death during renal injury. Here we focus on the regulation of actin organization during cisplatin-induced nephrotoxicity.

The pro-inflammatory cytokine tumor necrosis factor α (TNF-α) is involved in cisplatin-induced nephrotoxicity *in vivo* (14, 15). Recently, we showed that cisplatin-induced cell death of PTECs is aggravated by pre-exposure to TNF-α (16). This enhancement was associated with inhibition of TNF-α-induced nuclear factor κ B (NF-κB) activation by cisplatin. Interestingly, TNF-α mediated apoptosis has been associated with activation of the actin regulatory protein family of Rho GTPases in several cell lines (17). This Rho GTPase family, including amongst others, Cdc42, Rac, RhoA, and regulating the Rho kinase (ROCK) (18) and myosin light chain kinase (MLCK) (19), is the most important family of proteins responsible for the actin cytoskeletal network changes that occur during PTEC injury (20, 21). TNF-α has specifically been shown to induce the activation of the GTPases Cdc42, Rac and Rho (17, 22).

Here we investigated the involvement of TNF-α and downstream NF-κB signalling in the regulation of cisplatin toxicity through the control of actin cytoskeletal changes that occur during cisplatin cytotoxicity. We show that TNF-α aggravates cisplatin-induced disruption of actin stress fibres in association with reduction of focal adhesions and loss of cell-cell contacts, ultimately resulting in enhanced apoptosis. Intriguingly, knock-down of the NF-κB subunit RelB, but not other NF-kB family members, protected the cells against this synergistic apoptosis. This was associated with inhibition of the morphological changes induced by TNF-α. Gene array analysis revealed that knock-down of RelB was associated with an epithelial-to-mesenchymal (EMT)-like transition via up-regulation of snail2. Moreover, during cisplatin/TNF-α treatment, RhoA-pathway related gene expression, including Rhophilin and ARHGEF3, was increased. Inhibition of RhoA/ROCK signalling re-established the synergistic apoptosis with the cisplatin/TNF-α treatment in shRelB cells, indicating that TNF-α aggravated cisplatin-induced PTEC apoptosis via RelB-mediated RhoA/ROCK inactivation.

2. Material and methods

2.1. Reagents and antibodies

Mouse recombinant TNF-α was acquired from R&D Systems (Abingdon, UK). The selective ROCK inhibitor Y27632 was from Bio-Connect (Huissen, The Netherlands). The MLCK inhibitor ML-7 was from Enzo Life Sciences (Antwerpen, Belgium). cis-diamminedichloroplatinum(II) (cisplatin) was from Sigma-Aldrich (Zwijndrecht, The Netherlands). AnnexinV-Alexa488 was made as described (23). The antibodies against β-actin, RelA, NF-κB1 and RelB were from Santa Cruz (Tebu-Bio, Heerhugowaard, The Netherlands) and the phospho-specific JNK antibody (Thr183/Tyr185) was from New England Biolabs (Leusden, The Netherlands). The antibody against NF-κB2 was from Cell Signalling (Bioké, Leiden, The Netherlands). The antibody against β-catenin was from BD Biosciences (San Jose, CA, USA), the antibody against P-paxillin Y118 was from Biosource (Bleiswijk, The Netherlands) and rhodamine phalloidin was from Molecular probes (Breda, The Netherlands).

2.2. Cell culture

Immortalized proximal tubular cells (IM-PTECs) described previously (24) were cultured at 33°C in HK2 medium (DMEM/F12 medium (Invitrogen, Breda, The Netherlands) with 10% fetal bovine serum (Hyclone, Etten-Leur, The Netherlands), 5 µg/ml insulin and transferrin, 5 ng/ml sodium selenite (Roche), 20 ng/ml triiodo-thyrionine (Sigma-Aldrich), 50 ng/ml hydrocortisone (Sigma-Aldrich), and 5 ng/ml prostaglandin E1 (Sigma- Aldrich) with L-glutamine and antibiotics (both from Invitrogen) and mouse interferon-γ (IFN-γ) (1 ng/ml; R&D Systems)) in 5% CO2 and 95% air between passage 3 and 20. Prior to each experiment, the cells were differentiated into proximal tubular cells by culturing them for 4 days under restrictive conditions (at 37°C in the absence of IFN-γ). The cells were then plated in the appropriate assay plates and cultured for 2 more days. In total, IM-PTECs were cultured under restrictive conditions for 6 days, allowing the disappearance of SV40 activity and completion of differentiation (24).

2.3. Exposures

IM-PTECs were exposed to 20 µM cisplatin or vehicle in the presence or absence of TNF-α (8 ng/ml). Exposure to TNF-α was performed 30 minutes prior to cisplatin as previously described (16). Cells were pre-incubated with Y27632 and ML-7 inhibitors

30 minutes prior TNF-α.

2.4. Lentiviral knock-downs

Stable IM-PTECs with knock-down of each NF-κB member were generated using lentiviral shRNA vectors (Sigma-Aldrich, in collaboration with Rob Hoeben, Leiden University Medical Centre, The Netherlands) and selection with puromycin (1 μg/ml). The plasmid encoding non-target control SHC002 was used as a control, the plasmids encoding mouse RelA number TRCN55343 (CCGGGCGAATCCAGACCAACAATAACTCGAGTTATTGTTGGTCTGGATTCGCTTTTTG) and TRC55346 (CCGGCTGTCCTCTCACATCCGATTTCTCGAGAAATCGGATGTGAGAGGACAGTTTTTG), mouse RelB number TRC095314 (CCGGCGGTTCTCTTTGAGCCCATTTCTCGAGAAA TGGGCTCAAAGAGAACCGTTTTTG) and TRC095318 (CCGGCGTGACTGTCAATGTGTTCTTCTCGAGAAGAACACATTGACAGTCACGTTTTTG), mouse c-Rel number TRC042549 (CCGGCCATTGTTTCTAACCCAATTTCTCGAGAAATTGGGTTAGAAACAATGGTTTTTG) and TRC042550 (CCGGGCGACTTGAGTGCATCTAATTCTCGAGAATTAGATGCACTCAAGTCGC TTTTTG), mouse NF-κB1 number TRC009514 (CCGGCACTGCTTTGACTCACTCAATCTCGAGATTGAGTGAGTCAAAGCAGTGTTTTT), mouse NF-κB2 TRC012343 (CCGGCCTGTCTAATCGAAATCTTATCTCGAGATAAGATTTCGATTAGACAGGTTTTT) and TRC012346 (CCGGCGTCATTTATCACGCTCAGTACTCGAGTACTGAGCGTGATAAATGACGTTTTT) were used.

2.5. Live apoptosis

Real time induction of apoptosis was quantified using a live cell apoptosis assay previously described (23). Briefly, binding of annexin V-Alexa488 conjugate to phosphatidyl serine present on the membranes of apoptotic cells was followed in time by imaging the cells every hour after drug exposure with a BD Pathway 855 imager (Becton Dickinson, Erembodegem, Belgium). The total area of annexin V-Alexa488 fluorescence per image was quantified using Image Pro (Media Cybernetics, Bethesda, MD).

2.6. Western Blot

Cells were harvested as described (25). The samples were subjected to protein separation and blotted on Immobilon-P membranes (Millipore, Amsterdam, The Netherlands).The membranes were blocked overnight at 4°C in milk powder 5% (w/v) in Tris-buffered saline/Tween 20 (TBST-T). Primary antibody incubation was performed for one hour at room temperature followed by incubation with horseradish peroxidase-conjugated or Cy5-labeled secondary antibodies (Jackson Immunoresearch,

Newmarket, UK) in TBS-T for 1 h at room temperature. Protein signals were detected with ECL (GE Healthcare) followed by film detection for the NF-κB members or by visualization on the Typhoon 9400 imager (GE Healthcare, Diegem, Belgium) for β-actin.

2.7. Immunofluorescence

Cultured cells were immuno-stained for β-catenin, P-paxillin-Y118 and F-actin (Rhodamine/Phalloidin) followed by secondary antibody labelling (goat anti-mouse Alexa488-labeled, goat anti-rabbit Alexa488-labeled (Molecular Probes, Breda, The Netherlands) and goat anti-mouse Cy3-labeled (Jackson Immunoresearch, Newmarket, UK)). Hoechst 33258 (2 μg/ml) was used to visualize the nuclei. Cells were imaged using a Nikon TiE2000 confocal microscope (Nikon, Amstelveen, Netherlands). All antibodies were used with a 1:1000 dilution.

2.8. Quantitative analysis of cell-cell junctions and focal adhesions

β-catenin segmentation and quantification was performed using ImageJ 1.44i software, as previously described (12), by calculating the average area occupied by β-catenin fluorescence signal in the cell-cell junction region of each cell and expressing it as β-catenin junction size per nucleus. Focal adhesion quantification was performed using ImageJ 1.43h software. Segmentation of the two signals P-paxillin-Y118 and Hoescht was followed by artificial cell region border creation. With the segmented P-paxillin-Y118 and nucleus masks together with the reconstructed cell region border, several phenotypic measurements were derived including focal adhesion size, dispersion, orientation and number. A minimum of 3400 focal adhesions and 100 cells per conditions was used for the quantification. The FA size distribution was represented as empirical cumulative distribution function (CDF) curves using the cdfplot function of the MATLAB® software (MathWorks®, Eindhoven, The Netherlands). The empirical cdf F(x) is defined as the proportion of X values less than or equal to x.

2.9. Gene array analysis

IM-PTECs wt, control shRNA (shCtrl) cells and shRNA RelB (shRelB) cells were exposed to vehicle, cisplatin (20μM), TNF-α (8ng/ml) or cisplatin in combination with TNF-α for 8 hours. Three replicates for each treatment were used. Total RNA was isolated from cells using an RNeasy® Mini Kit (Qiagen, Venlo, The Netherlands) according to the

manufacturer's protocol. RNA concentration was determined by absorbance at 260 nm (Nanodrop Technologies, Montchanin, DE, USA), and the integrity of the RNA was checked using an Agilent 2100 Bioanalyzer (Agilent Technologies, Palo Alto, CA, USA). The synthesis of labelled cRNA and hybridization steps were performed by Service XS (Leiden, The Netherlands). Briefly, 100 ng of RNA was used to synthesize Biotin-labeled cRNA with the Affymetrix 3´ IVT Express Labeling Kit. The resulting labelled cRNA was quantified by absorbance at 260 nm (Nanodrop) and 6 µg was hybridized on an Affymetrix 24 all-in HT MG 430 PM Array plate following the procedures recommended by the manufacturer. After hybridization, the microarray slide was washed, dried, and scanned using the Hybridization, Wash and Stain Kit #901530 compatible with Affymetrix protocols. The Affymetrix Command Console (v3.0) and Expression Console software (v1.1) were used to analyze the performance of the washing, staining and scanning of the chips.

Subsequently, the raw intensity data were normalized with BRB array Tools software (developed by Dr. Richard Simon and BRB-ArrayTools Development Team; http://linus.nci.nih.gov/BRB-ArrayTools.html) using the Robust Multichip Average (RMA) method. Significantly differentially expressed genes (false discovery rate FDR≤ 0.1) between the various experimental conditions were identified with a one-way blocked ANOVA test. A randomized blocked design was chosen to control for the different days that the replicate experiments were run. The ANOVA test was followed by calculation of the FDRs according to Benjamin and Hochberg (26). Since only one differentially expressed gene was found between wt and shCtrl cells, they were pooled to increase the statistical power of the analysis. Only probes with expression levels of 1.5-fold change or more relative to wt+shCtrl cells were selected for further analysis.

Commonly deregulated genes between the different groups were identified by Venn diagrams. Pathway analysis of the selected genes was performed using the GeneGoMetacore™ pathway analysis software (GeneGo, MI, USA). Heatmap representations were performed using the MultiArray Viewer software. The complete data set will be submitted to ArrayExpress (EMBL-European Bioinformatics Institue, Hinxton, England; http://wwww.ebi.ac.uk/arrayexpress) and will be available for public download shortly. Accession number referencing this data set will be available on the GEO database website (http://www.ncbi.nlm.nih.gov/geo/).

2.10. Statistical procedures

All data are expressed as mean ± standard error of the mean (S.E.M.). Statistical

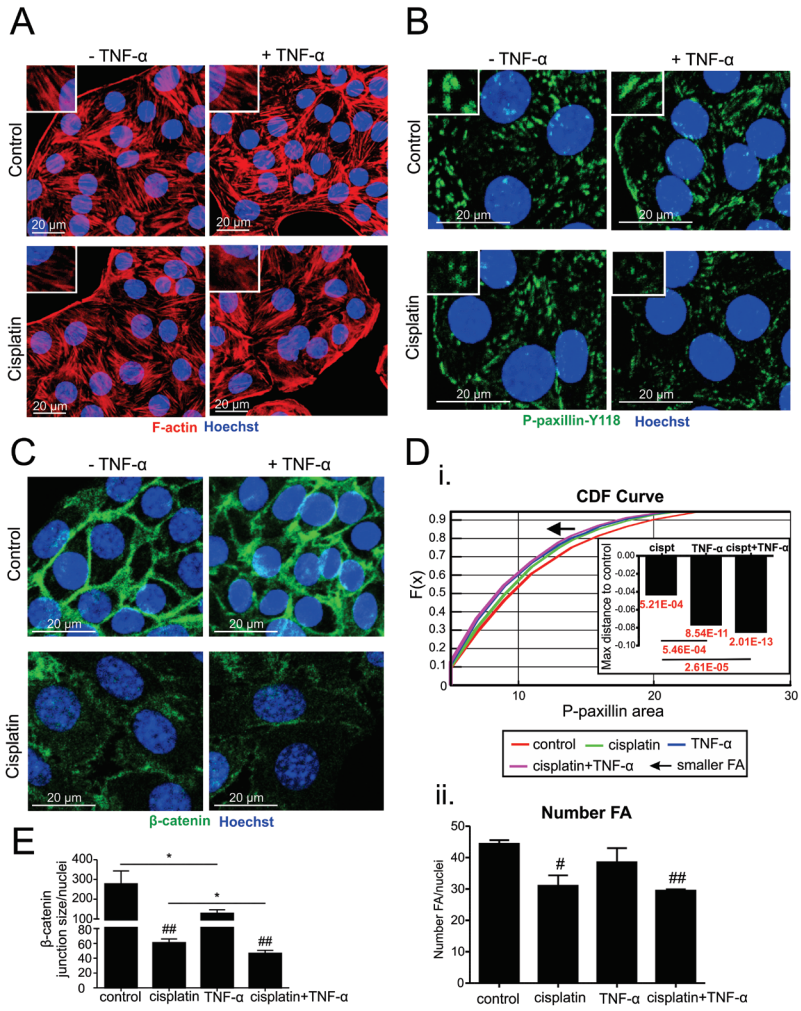


Figure 1. TNF-α aggravates cisplatin-induced disruption of stress fibres, cell-ECM adhesion and cell-cell contacts. IM-PTECs were exposed to cisplatin (20 µM) and/or TNF-α (8 ng/ml) for 8 hours and immunostained to visualize the actin cytoskeleton, the focal adhesions and cell-cell adhesions. Cells were imaged using a Nikon TiE2000 confocal microscope. The effect of treatment on the actin cytoskeleton was visualized by staining of F-actin with rhodamine phalloidin (red) (A). The effect of treatment on focal adhesions (FA) was assessed by staining of P-paxillin-Y118 (green)(B). Quantification of P-paxillin was performed. The CDF curve indicates the direction of the changes in focal adhesion size with the different treatments. A KS test was performed relative to control treatment and indicates the differences observed in P-paxillin size between cisplatin and/or TNF-α treated cells and vehicle-treated cells. The p-values obtained are indicated in red. The number of focal adhesion was also assessed by quantifying P-paxillin fluorescence per cell (D). Cell-cell contacts disturbances after treatment were assessed by staining the adherens junction protein β-catenin (green) (C), which was quantified by assessing the average area occupied by β-catenin per cell (E). For all images, the nuclei were stained with Hoechst (blue) (A, B and C). Images of shCtrl cells and shRelB cells have the same scale as indicated in the images in the bottom right corner. The data are representative of three independent experiments and expressed as mean ± S.E.M. * P ≤ 0.05 and # P ≤ 0.05, # # P ≤ 0.01 compared to vehicle-treated cells.

significance was determined by GraphPad Prism using an unpaired two-tailed t-test. Data from focal adhesion quantification were analysed using the non-parametric Kolmogorov-Smirnow (KS) test via the MATLAB® software (MathWorks®, Eindhoven, The Netherlands) which computes test statistics that are derived from the empirical cdf. The CDF curves are represented and the level of confidence is indicated by P-values in the figures.

3. Results

3.1. TNF-α aggravates cisplatin-induced disruption of stress fibres, cell-ECM and cell-cell adhesion

In a recent study we showed that TNF-α enhanced cisplatin-induced cell death in immortalized proximal tubular epithelial cells (IM-PTECs) (16). As cisplatin alone is known to induce actin reorganization, and loss of cell-cell and cell-ECM adhesion prior to apoptosis of renal tubular cells (7, 11-13), we determined whether TNF-α could promote these events. IM-PTECs were exposed to cisplatin (20 μM) and/or TNF-α (8 ng/ml) for 8 hours and thereafter immuno-stained to visualize the actin cytoskeleton, the focal adhesions and cell-cell adhesions. Treatment of the cells with TNF-α alone enhanced actin fibre formation in particular at cell-cell junctions (Fig. 1A), but diminished the average size of focal adhesions (Fig. 1B and D) and reduced the accumulation of β-catenin molecules at the cell membrane (Fig. 1C and E). This effect of TNF-α aggravated the reorganization and disruption of the stress fibres (Fig. 1A), the loss of focal adhesions (Fig. 1B and D) and the loss of β-catenin at the cell–cell contacts (Fig. 1C and E) caused by cisplatin treatment alone. These data show that prior to the onset of apoptosis, TNF-α aggravates the cytoskeletal and cell adhesion reorganization induced by cisplatin alone.

3.2. RelB knock-down suppresses cisplatin/TNF-α synergistic apoptosis

TNF-α activates NF-κB signalling. Furthermore, NF-κB signalling can affect the actin cytoskeletal organization (27). The NF-κB transcription factor comprises five different members: RelA, RelB, NF-κB1, NF-κB2 and c-Rel (28). Our next goal was therefore to determine which NF-κB subunit could contribute to the TNF-α mediated aggravation of both cisplatin-induced cytoskeletal reorganization and cell death. We therefore first systematically generated knock-down IM-PTEC cell lines using five individual lenti-viral

shRNA targeting each individual NF-κB family member. Knock-down was confirmed using Western blotting (Supplemental Fig. 1A). For NF-κB1 only one, instead of two out of 5 shRNA lentiviral vectors resulted in a sufficient and reliable protein knock-down. Due to its very weak expression in our IM-PTECs known from previous Affymetrix array data (16), c-Rel was not considered for further investigation.

Next, we investigated the effect of the knock down of each NF-κB member on cisplatin- and cisplatin/TNF-α-induced apoptosis. All cell lines were exposed to cisplatin (20 μM) and/or TNF-α (8 ng/ml) and cell death was measured using live apoptosis imaging. RelA and NF-κB1 knock-down increased cisplatin- and cisplatin/TNF-α-induced apoptosis (Fig. 2A); suggesting a role for the RelA/p50 NF-κB dimer to act in survival signalling. Interestingly, for both NF-κB2 knock-down cell lines, an increased cisplatin-induced apoptosis was observed, while cisplatin/TNF-α-induced apoptosis was unaffected (Fig. 2A). This observation indicates that in our IM-PTECs, NF-κB2-based NF-κB signalling protects the cells from cisplatin-induced apoptosis. Importantly, knock-down of RelB using two independent shRNAs, suppressed the cisplatin/TNF-α-induced synergistic apoptosis without affecting cisplatin-induced apoptosis (Fig. 2A). This suggests that RelB is the only NF-κB family member that is key in the regulation of the TNF-αmediated enhancement of cisplatin-induced apoptosis. Of critical relevance, TNF-α itself increased expression of RelB both at the gene as well as protein expression level, which was not affected by cisplatin (Fig. 2B and C). Together, these data indicate that the NF-κB family member RelB is directly involved in the pro-apoptotic activity of TNF-α and, thereby, enhances cisplatin-induced apoptotic cell death.

3.3. RelB knock-down inhibits cisplatin/TNF-α-induced cell adhesion and actin cytoskeleton changes

Next, we determined whether depletion of RelB also affected the TNF-α- and cisplatin-mediated changes in actin cytoskeletal network, cell-matrix adhesions and cell-cell contacts. Cisplatin caused loss of F-actin organization and cell matrix and cell-cell adhesions in shCtrl cells as expected (Fig. 3A-D), which was further enhanced by TNF-α. Knock-down of RelB resulted in some morphological changes compared to both wt and shCtrl cells. shRelB cells were more spread with a reorganization of stress fibres around the nucleus, larger focal adhesions and a reduced cortical-actin network. In addition, a loss in cell-cell contact formation was observed as indicated by the disappearance of β-catenin at the cell-cell border (Fig. 3A-E). Although we expected these changes to influence cisplatin-induced renal cell death, no significant changes

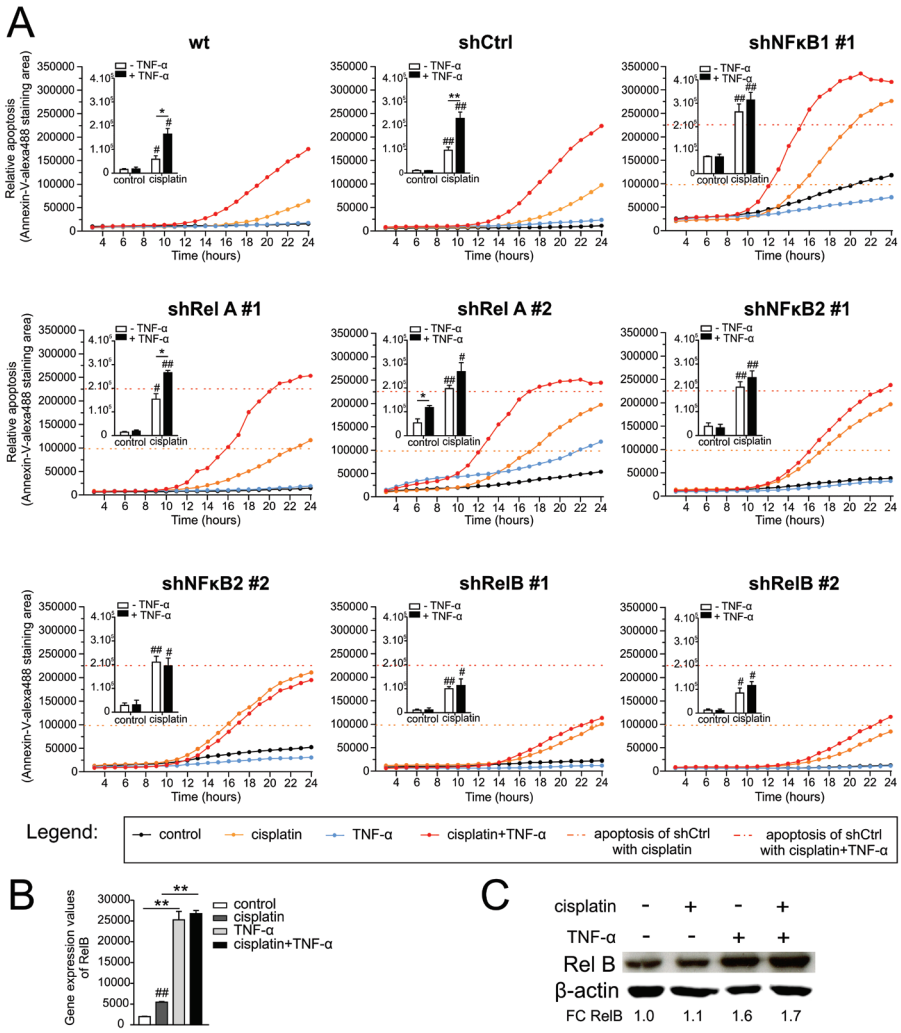


Figure 2. RelB knock-down suppresses cisplatin/TNF-α synergistic apoptosis. IM-PTEC cell lines with knock-down for each NF-κB family member (NF-κB1, NF-κB2, RelA and RelB) were generated using lenti-viral shRNA (see materials and methods). Knock-down cells were exposed to cisplatin (20 μM) and/or TNF-α (8 ng/ml). Cell death was followed over time using Annexin V-Alexa488 staining and automated imaging. Both apoptosis overtime and endpoints are represented. The dashed orange and red lines indicate the amount apoptosis observed with shCtrl cells after cisplatin or cisplatin/TNF-α treatment respectively (A). After cisplatin (5 μM) and/or TNF-α (8 ng/ml) treatment for 8 hours, the gene expression (B) and protein (C) levels of RelB were assessed. Gene expression values were obtained from previous Affymetrix gene array data (16) (B) and protein levels were assessed by Western blotting (C). β-actin was used as a loading control and the quantification indicated is the mean of three independent experiments (C). The data are representative of three independent experiments and expressed as mean± S.E.M. * P ≤ 0.05, ** P ≤ 0.01 and # P ≤ 0.05, # # P ≤ 0.01 compared to vehicle-treated cells.

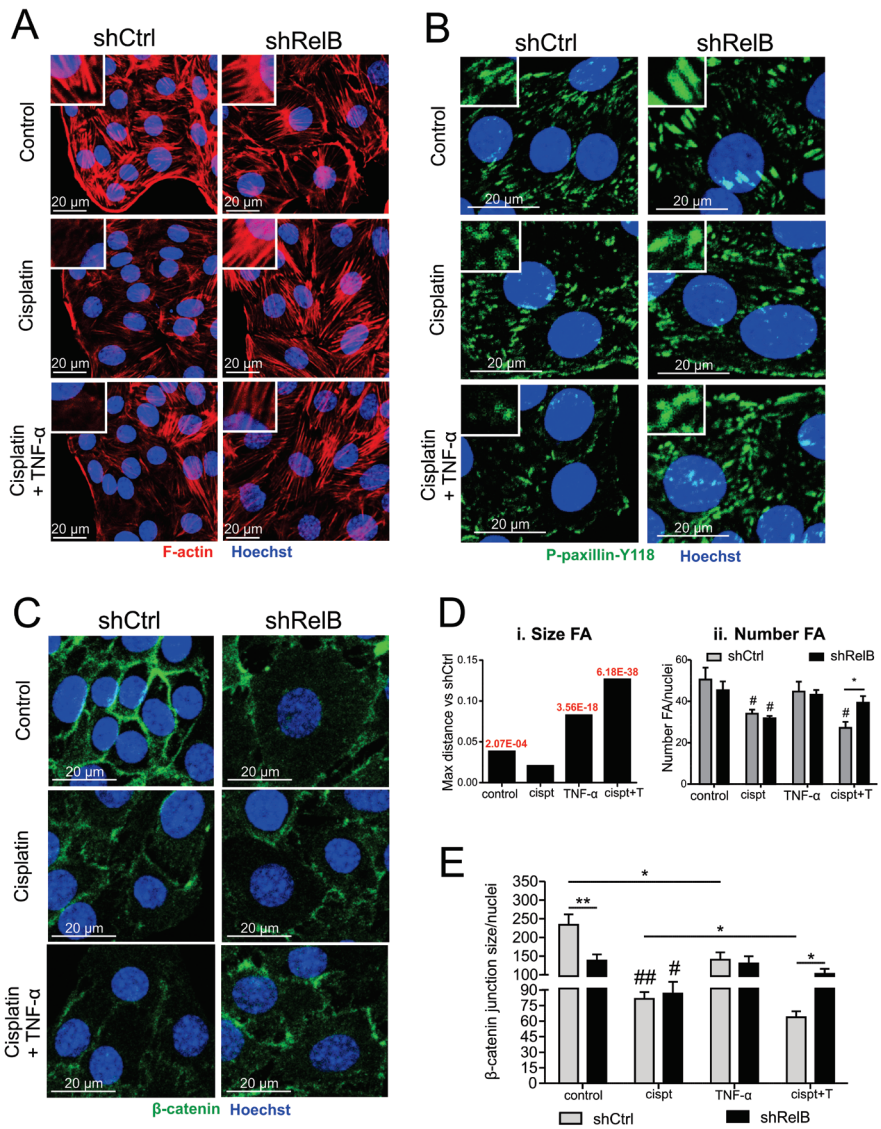


Figure 3. RelB knock-down inhibits cisplatin/TNF-α-induced cell adhesion and actin cytoskeleton changes. shCtrl and shRelB cells were exposed to cisplatin (20 μM) and/or TNF-α (8 ng/ml) for 8 hours and immuno-stained to visualize the actin cytoskeleton, focal adhesions and cell-cell adhesions. Cells were imaged using a Nikon TiE2000 confocal microscope. The effect of RelB knock-down on actin cytoskeleton was visualized by staining of F-actin with rhodamine phalloidin (red) (A). The effect of RelB knock-down on focal adhesions was assessed by staining of P-paxillin-Y118 (green) (B). Cell-cell contacts disturbances after treatment were assessed by staining the adherens junction protein β-catenin (green) (C). Quantification of P-paxillin (D) and β-catenin (E) was performed as described under Fig. 1 and materials and methods. For all images, the nuclei were stained with Hoechst (blue) (A, B and C). Images of shCtrl cells and shRelB cells have the same scale as indicated in the images in the bottom right corner. cispt=cisplatin, cispt+TNF-α and cispt+T=cisplatin+TNF-α. The data are representative of three independent experiments and expressed as mean ± S.E.M. * P ≤ 0.05 and # P ≤ 0.05, # # P ≤ 0.01 compared to vehicle-treated cells.

were observed between DMSO and cisplatin-treated cells. However, in sharp contrast to shCtrl cells, treatment of shRelB cells with cisplatin/TNF-α did not result in drastic morphological changes: cisplatin/TNF-α treated shRelB cells maintained their actin organization and did not show significant changes in focal adhesion size and number (Fig. 3A-D and Supplemental Fig. 2A) coinciding with the protection of the cells. Furthermore, although slightly diminished, β-catenin containing cell-cell adhesions remained largely intact during cisplatin/TNF-α treatment of shRelB cells compared to untreated cells (Fig. 3C and E). Together, these data indicate that RelB-mediated signalling is essential in the nephrotoxic cytoskeletal reorganization in association with the onset of cell death during cisplatin/TNF-α treatment.

3.4. RelB knock-down leads to EMT-like driven cytoskeletal reorganization

To obtain detailed insight into the pathways involved in the actin cytoskeleton changes and the suppression of the synergistic apoptosis observed in shRelB cells, transcriptomic analysis was performed. Wt, shCtrl and shRelB cells were exposed to cisplatin (20 μM) and/or TNF-α (8 ng/ml) for 8 hours, a time point at which cell death did not yet occur (Fig. 2). Since wt cells and shCtrl cells only had one statistically different gene (Neurog3) with a FDR≤ 0.1, we pooled the datasets to increase the statistical power of our gene array analysis. We first analysed the effect of RelB knock-down on gene expression changes under control conditions. Gene expression changes with ≥ 1.5 fold-change and FDR ≤ 0.1 for shRelB#1 and #2 cells compared to wt+ shCtrl cells were considered for further analysis. A total of 800 genes for shRelB#1 and 698 genes for shRelB#2 were identified with our selection criteria and 388 genes were common for both shRelB cell lines (Fig. 4A). A pathway analysis was then performed on these common genes under control conditions using the GeneGoMetacore™ pathway analysis software. The top 7 significantly different pathways were all related to cytoskeletal and cell adhesion changes as well as induction of an EMT (Fig. 4B). The most prominent cytoskeleton and cell adhesion-related genes that were up-regulated by RelB knock-down included actin (Actb), myosin IIB (Myh10), the gene encoding the tight junction-related protein cingulin (Cgn), the cell adhesion-related genes collagen type IV alpha 1 (Col4a1) and serpine 2 as well as the genes encoding the Cdc42 regulating proteins Cdc42 small effector 1 (Cdc42se1) and Par6 (Pard6g) (Fig. 4C). In contrast, Vcan, encoding the cell adhesion protein versican was down-regulated in shRelB cells (Fig. 4C). In addition, one of the key EMT inducing genes, Snai2,

encoding the protein Snail2, was more than 2 fold up-regulated in both shRelB cell lines (Fig. 4C), suggesting that the cytoskeletal changes described above could well be a consequence of a Snai2-induced EMT-like switch of the PTEC cells. Other EMT-related transcription factors, including Twist, were not affected.

3.5. RelB knock-down leads to Rho kinase pathway activation during cisplatin/TNF-α treatment

We next evaluated which pathways were affected by RelB knock-down under TNF-α, cisplatin or TNF-α/cisplatin conditions. Gene expression changes with ≥ 1.5 fold-change and FDR≤ 0.1 for shRelB#1 and shRelB#2 cells compared to wt+ shCtrl cells were considered for further analysis. Comparing differentially expressed genes between treatments resulted in identification of 21 and 17 uniquely changing genes for cisplatin and TNF-α treatments respectively compared to 118 and 70 uniquely changing genes for vehicle and cisplatin/TNF-α treatments respectively (Supplemental Fig. 3 and Supplemental Table 1).

To identify pathways by which RelB controlled the synergistic apoptosis induced by cisplatin/TNF-α treatment, pathway analysis was performed on the common genes in cells treated with the combined cisplatin/TNF-α treatment using the GeneGoMetacore™ pathway analysis software. A total of 782 genes for shRelB#1 and 462 genes for shRelB#2 were identified under these treatment conditions and 278 genes were common for both shRelB cell lines (Fig. 5A) comprising the 70 unique genes (Supplemental Fig. 3 and Supplemental Table 1). Pathway analysis showed that also under cisplatin/TNF-α conditions, the top significantly different pathways were all related to cytoskeletal and cell adhesion changes as well as induction of an EMT (Fig. 5B). The main genes involved in cell adhesion included the Ras-related protein 1a (Rap1a), the Eph receptor B3 (Ephb3) and the gap junction protein β2 (Gjb2) (Fig. 5C) of which expression of Rap1a and Gjb2 was specifically changed under cisplatin/TNF-α conditions. Interestingly, the EMT gene snai2 was slightly induced in shCtrl cells; yet, depletion of RelB allowed an even further induction of snai2 expression after cisplatin treatment, which was approximately four times higher than under shCtrl conditions and independent of TNF-α (Fig. 5C). In addition, RhoGTPase pathway activation was observed in shRelB IM-PTECs (Fig. 5B), including up-regulation of Rho guanine nucleotide exchange factor 3 (Arhgef3) and rhophilin 1 (Rhpn1) (Fig. 5C). Together these data suggest a key role for RelB to suppress a stress-induced cytoskeletal reorganization response, which is likely part of an EMT-like program.

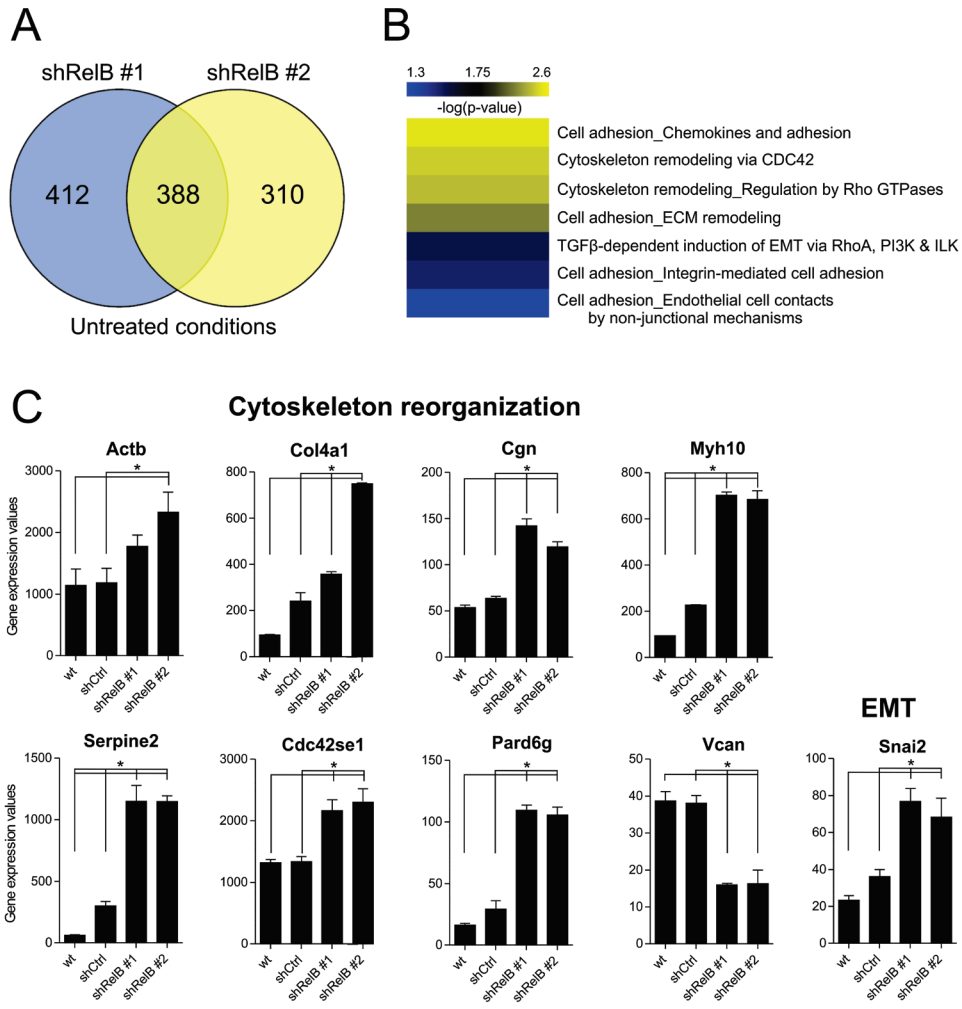


Figure 4. RelB knock-down leads to EMT-like driven cytoskeletal rearrangements in vehicle-treated cells. shCtrl and shRelB cells were exposed to cisplatin (20 μM) and/or TNF-α (8 ng/ml) for 8 hours. Following hybridization and RMA normalization, the genes with ≥ 1.5 fold-change and FDR≤ 0.1 for shRelB #1 and #2 cell lines compared to wt+ shCtrl cells in control conditions were further selected. A Venn diagram was made comparing both shRelB cell lines in control conditions (A). Using the Metacore™ software, pathway analysis was performed on the genes commonly regulated in both shRelB cell lines in control conditions. The top pathways are represented in a heatmap (B). The gene expression changes of genes involved in cytoskeleton organization and EMT are represented for wt and shCtrl as well as both shRelB cell lines in control conditions. The data are representative of three independent experiments and expressed as mean ± S.E.M. * P ≤ 0.05 (C).

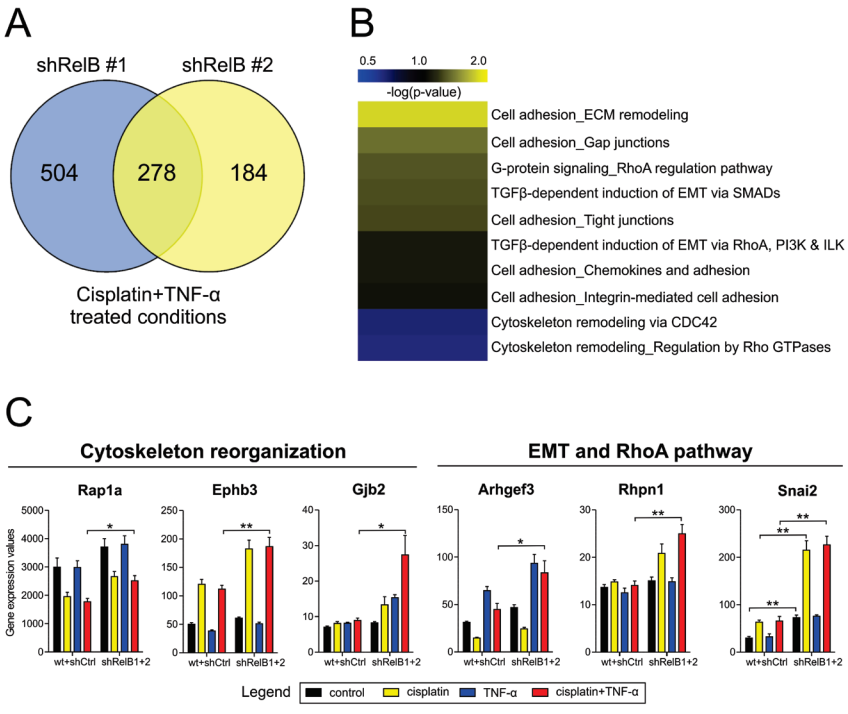


Figure 5. RelB knock-down is associated with up-regulation of RhoA pathway related genes during cisplatin/TNF-α treatment. shCtrl and shRelB cells were exposed to cisplatin (20 μM) and/or TNF-α (8 ng/ml) for 8 hours. Following hybridization and RMA normalization, the genes with ≥ 1.5 fold-change and FDR≤ 0.1 for shRelB#1 and #2 cell lines compared to wt+ shCtrl cells after cisplatin/TNF-α treatment were further selected. A Venn diagram was made comparing both shRelB cell lines (A). Using the Metacore™ software, pathway analysis was performed on the genes commonly regulated in both shRelB cell lines with cisplatin/TNF-α treatment. The top pathways are represented in a heatmap (B). The gene expression changes of genes involved in cell adhesion, EMT and the RhoA pathway are represented for wt-shCtrl cells combined and both shRelB cell lines combined in cisplatin/TNF-α treated conditions The statistical significance is indicated only for the conditions where for both shRelB#1 and #2 the fold-change was ≥1.5. The data are representative of three independent experiments and expressed as mean ± S.E.M. * P ≤ 0.05 and ** P ≤ 0.05 (C).

3.6. RelB knock-down protects against cisplatin/TNF-α treatment in a Rho kinase dependent manner

The Rho GTPase family is the most important family of proteins responsible for the regulation of the actin cytoskeletal network in cells and it is known to be involved in PTEC injury (19, 20). Given the changes observed in the expression of some Rho-GTPase

family members in shRelB cells, we determined whether RelB knock-down protects the IM-PTECs against cisplatin/TNF-α induced synergistic cell death via activation of the Rho GTPase pathway. Therefore we inhibited one of the key downstream components, Rho kinase using the Y27632 inhibitor. Cells were pre-exposed for 30 minutes with the ROCK inhibitor and thereafter treated with cisplatin (20 μM) and/or TNF-α (8 ng/ml). Y27632 caused disruption of stress fibres formation in both shCtrl and shRelB cells (Fig. 6A). This disruption of the stress fibres was accompanied by an enhancement of apoptosis in shCtrl cells after both cisplatin and cisplatin/TNF-α treatment (Fig. 6B). In

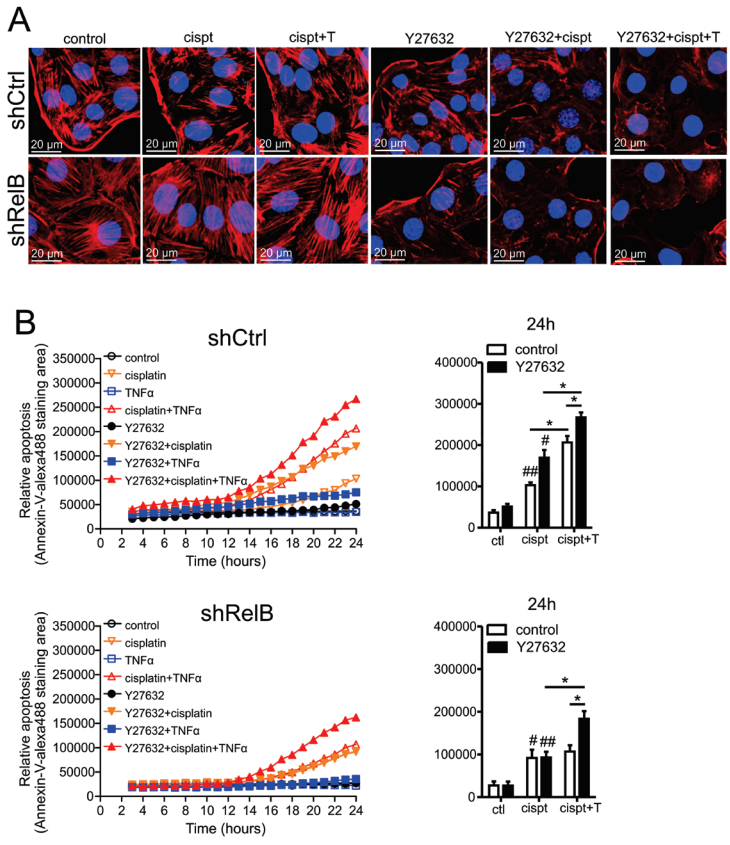


Figure 6. RelB knock-down protects against cisplatin/TNF-α treatment in a Rho kinase dependent manner. shCtrl and shRelB cells were pre-exposed to the ROCK inhibitor Y27632 for 30 minutes prior to cisplatin (20 μM) and/or TNF-α (8 ng/ml). After 8 hours of exposures to cisplatin and/or TNF-α in combination with the ROCK inhibitor, actin was visualized by staining of F-actin with rhodaminephalloidin (red). The nuclei were visualized with Hoechst staining (blue). Images of both shCtrl cells and shRelB cells have the same scale as indicated in the images in the bottom right corner (A). Cell death after ROCK inhibition was followed over time using Annexin V-Alexa488 staining and automated imaging (B). ctl=control, cispt=cisplatin and cispt+T=cisplatin+TNF-α. The data are representative of three independent experiments and expressed as mean ± S.E.M. * P ≤ 0.05 and # P ≤ 0.05, # # P ≤ 0.01 compared to vehicle-treated cells.

shRelB cells, the apoptosis was only increased with cisplatin/TNF-α treatment and not with cisplatin treatment alone (Fig. 6B).

These data are indicative for mechanism whereby RelB knock down confers protection against cisplatin/TNF-α treatment in a Rho kinase dependent manner.

4. Discussion

In the present study we demonstrate that TNF-α aggravated the cisplatin-induced changes in the actin cytoskeleton and cell adhesions that occur prior to the onset of apoptosis. Knock-down of the NF-κB family member RelB abrogated both the synergistic cisplatin/TNF-α-induced apoptosis as well as the changes in actin cytoskeleton and cell adhesions. RelB knock down resulted in an enhancement of the expression of Rho GTPase-related actin cytoskeletal regulators in association with a snai2-related EMT-like program. Likewise, a Rho kinase inhibitor, Y27632, reversed the cytoprotective effect of the RelB depletion.

Although the transcription factor NF-κB has been associated with morphological changes that occur prior to apoptosis (27), the role of the family member RelB in Rho kinase regulation in relation to cell death has never been described before. Our study showed that up-regulation of RelB is responsible for the synergistic apoptosis induced by cisplatin/TNF-α treatment. This observation is contradictory to studies using thymocytes and cancer cells, in which RelB is involved in anti-apoptotic signalling (29-31); these effects were independent of TNF-α signalling. Moreover, different transcriptional programs may be activated by RelB in immune and cancer cells, compared to renal cells. Jacque et al. showed in mouse embryonic fibroblasts that although RelB entered the nucleus in response to TNF-α, it could not bind to DNA due to repression by RelA (32). In our IM-PTECs TNF-α-induced RelA translocation was inhibited by cisplatin/TNF-α treatment (16). Furthermore, RelB expression was up-regulated during TNF-α treatment (Fig. 2B-C). It could well be that the increase in apoptosis in our cells is due to the combination of RelB up-regulation and RelA translocation inhibition, thereby resulting in a different transcriptional program than the one occurring in immune and cancer cells. Additionally, other kinases regulating the cytoskeletal organization such as Src could be involved. v-Src has been shown to regulate the activation of RelB via accelerating IκB proteolysis in fibroblasts (33) and TNF-α increased Src activity in intestinal epithelial cells (34). It could well be that in our cells, the increased RelB activity observed with TNF-α and cisplatin/TNF-α treatments is due to increased Src activation.

Transcriptomic analysis revealed activation of the RhoA/Rho kinase pathway in shRelB cells during treatment of the cells with cisplatin/TNF-α via increased gene expression of ARHGEF3 and rhophillin 1. ARHGEF3 has been shown to activate RhoA and RhoB specifically leading to assembly of stress fibres and thereby enlargement of focal adhesions in a Rho kinase-dependent manner (35). Rhophilin 1 interacts strongly with GTP-bound RhoA, but its exact role in cytoskeletal organization remains elusive (36, 37). Their role in apoptosis is unknown. Using the Rho kinase inhibitor we showed that RhoA pathway activation was crucial for cisplatin/TNF-α-induced synergistic apoptosis. It is well known that depending on the cell type and stimulus used, activation of the RhoA/ROCK pathway can either lead to apoptosis or cell survival. For example, ROCK inhibition enhanced cisplatin-induced cytotoxicity of lung carcinoma cells through focal adhesion kinase (FAK) suppression-independent mechanism (38), while it attenuated I/R-induced renal injury in an *in vivo* model (39). In addition, several other studies indicated a protective role of ROCK in several cell types including epithelial, cancer, and endothelial cells as well as *in vivo* (40). Yet, to the best of our knowledge, the role of ROCK signalling in cisplatin-induced apoptosis in renal cells remained thus far unknown.

In addition to RhoA and ROCK pathway activation, our transcriptomic analysis demonstrated up-regulation of the EMT-regulatory gene snail2 in shRelB cells, which corresponded with the EMT-like switch observed in these cells. Since TNF-α strongly induces RelB expression (Fig. 2C), this may suppress a cytoprotective snai2-based EMT-like switch initiated by cisplatin. RhoA pathway activation was shown to be a key step in renal EMT, leading to trans-differentiation of renal tubular cells to fibroblasts (41, 42). It has been shown that renal regeneration during and after toxicant- or I/R-induced renal failure occurred by transformation of epithelial cells into fibroblasts via EMT. During an EMT, cells may acquire new mesenchymal markers such as vimentin, alpha smooth muscle actin (α-SMA), S100 calcium binding protein A4 (S100A4), the transcription factor Snail and N-cadherin (42). Although Snail was up-regulated over 2-fold, no changes occurred in gene expression of the mesenchymal markers vimentin, desmin, collagen I, fibronectin and N-cadherin. α-SMA gene expression was only increased in the shRelB#2 cells showing the highest knock-down but not in the shRelB#1 cells, while the S100A4 gene expression was down-regulated in both shRelB cell lines. Therefore, RelB knock-down did not induce a complete traditional EMT in IM-PTECs, but this partial EMT accompanied with RhoA/Rho kinase activation was sufficient to confer protection against the synergistic apoptosis induced by cisplatin/TNF-α treatment. In contrast to our data, Wang et al. showed that RelB expression was

required to maintain the mesenchymal phenotype of breast cancer cells (31).The link between RhoA/ROCK pathway activation and RelB in this process is not yet clear.

Lastly, our transcriptomic analysis revealed specific and significant changes in the expression of the cell-cell proteins Rap1a and Gjb2 in cisplatin/TNF-α-treated shRelB cells. We have previously shown that Rap1a preserved cell-cell junctions and protected against cisplatin-induced apoptosis in proximal tubular cells (12). Gjb2 is part of the connexins that could be involved in the proximal tubular cells in the formation of hemi-channels regulating renal sodium, potassium, and water handling (43). In mice, knock-out of GJB2 has been shown to responsible for cochlear cell apoptosis, so it could be that this connexin has also a protective role in renal cells (44).

In conclusion, our observations suggest that TNF-α-induced up-regulation of RelB expression is responsible for the cisplatin/TNF-α-induced synergistic apoptosis and show, for the first time, the role of RelB in renal EMT-induction and RhoA/ROCK-mediated cytoskeletal regulation as a protective mechanism.

Acknowledgements

This work was performed as part of the Netherlands ToxicogenomicsCenter (NTC)/ Netherlands Genomics Initiative supported by the Dutch Organization for Scientific Research (NWO) grant nr. 050-06-510 and the Dutch Top Institute Pharma project grant D3-201.

References

1. Thadhani R, Pascual M, Bonventre JV. Acute renal failure. The New England journal of medicine 1996;334:1448-1460.

2. Cordes N. Integrin-mediated cell-matrix interactions for prosurvival and antiapoptotic signaling after genotoxic injury. Cancer letters 2006;242:11-19.

3. Gailit J, Colflesh D, Rabiner I, Simone J, Goligorsky MS. Redistribution and dysfunction of integrins in cultured renal epithelial cells exposed to oxidative stress. The American journal of physiology 1993;264:F149-157.

4. Zuk A, Bonventre JV, Brown D, Matlin KS. Polarity, integrin, and extracellular matrix dynamics in the postischemic rat kidney. The American journal of physiology 1998;275:C711-731.

5. Pabla N, Dong Z. Cisplatin nephrotoxicity: mechanisms and renoprotective strategies. Kidney international 2008;73:994-1007.

6. Van de Water B, Jaspers JJ, Maasdam DH, Mulder GJ, Nagelkerke JF. In vivo and in vitro detachment of proximal tubular cells and F-actin damage: consequences for renal function. The

American journal of physiology 1994;267:F888-899.

7. Kruidering M, van de Water B, Zhan Y, Baelde JJ, Heer E, Mulder GJ, Stevens JL, et al. Cisplatin effects on F-actin and matrix proteins precede renal tubular cell detachment and apoptosis in vitro. Cell death and differentiation 1998;5:601-614.

8. Qin Y, Alderliesten MC, Stokman G, Pennekamp P, Bonventre JV, de Heer E, Ichimura T, et al. Focal adhesion kinase signaling mediates acute renal injury induced by ischemia/reperfusion. The American journal of pathology 2011;179:2766-2778.

9. van de Water B, Nagelkerke JF, Stevens JL. Dephosphorylation of focal adhesion kinase (FAK) and loss of focal contacts precede caspase-mediated cleavage of FAK during apoptosis in renal epithelial cells. The Journal of biological chemistry 1999;274:13328-13337.

10. van de Water B, Houtepen F, Huigsloot M, Tijdens IB. Suppression of chemically induced apoptosis but not necrosis of renal proximal tubular epithelial (LLC-PK1) cells by focal adhesion kinase (FAK). Role of FAK in maintaining focal adhesion organization after acute renal cell injury. The Journal of biological chemistry 2001;276:36183-36193.

11. van de Water B, Tijdens IB, Verbrugge A, Huigsloot M, Dihal AA, Stevens JL, Jaken S, et al. Cleavage of the actin-capping protein alpha -adducin at Asp-Asp-Ser-Asp633-Ala by caspase-3 is preceded by its phosphorylation on serine 726 in cisplatin-induced apoptosis of renal epithelial cells. The Journal of biological chemistry 2000;275:25805-25813.

12. Qin Y, Stokman G, Yan K, Ramaiahgari S, Verbeek F, de Graauw M, van de Water B, et al. cAMP signalling protects proximal tubular epithelial cells from cisplatin-induced apoptosis via activation of Epac. British journal of pharmacology 2012;165:1137-1150.

13. Imamdi R, de Graauw M, van de Water B. Protein kinase C mediates cisplatin-induced loss of adherens junctions followed by apoptosis of renal proximal tubular epithelial cells. The Journal of pharmacology and experimental therapeutics 2004;311:892-903.

14. Ramesh G, Reeves WB. TNF-alpha mediates chemokine and cytokine expression and renal injury in cisplatin nephrotoxicity. The Journal of clinical investigation 2002;110:835-842.

15. Ramesh G, Reeves WB. TNFR2-mediated apoptosis and necrosis in cisplatin-induced acute renal failure. American journal of physiology. Renal physiology 2003;285:F610-618.

16. Benedetti G, Fredriksson L, Herpers B, Meerman J, van de Water B, de Graauw M. TNF-α-mediated NF-κB Survival Signaling Impairment by Cisplatin Enhances JNK Activation Allowing Synergistic Apoptosis of Renal Proximal Tubular Cells. Biochemical pharmacology 2012.

17. Mathew SJ, Haubert D, Kronke M, Leptin M. Looking beyond death: a morphogenetic role for the TNF signalling pathway. Journal of cell science 2009;122:1939-1946.

18. Leung T, Manser E, Tan L, Lim L. A novel serine/threonine kinase binding the Ras-related RhoA GTPase which translocates the kinase to peripheral membranes. The Journal of biological chemistry 1995;270:29051-29054.

19. Amano M, Ito M, Kimura K, Fukata Y, Chihara K, Nakano T, Matsuura Y, et al. Phosphorylation and activation of myosin by Rho-associated kinase (Rho-kinase). The Journal of biological chemistry 1996;271:20246-20249.

20. Kroshian VM, Sheridan AM, Lieberthal W. Functional and cytoskeletal changes induced by sublethal injury in proximal tubular epithelial cells. The American journal of physiology 1994;266:F21-30.

21. Raman N, Atkinson SJ. Rho controls actin cytoskeletal assembly in renal epithelial cells during ATP depletion and recovery. The American journal of physiology 1999;276:C1312-1324.

22. Puls A, Eliopoulos AG, Nobes CD, Bridges T, Young LS, Hall A. Activation of the small GTPase Cdc42 by the inflammatory cytokines TNF(alpha) and IL-1, and by the Epstein-Barr virus transforming protein LMP1. Journal of cell science 1999;112 (Pt 17):2983-2992.

23. Puigvert JC, de Bont H, van de Water B, Danen EH. High-throughput live cell imaging of

apoptosis. Curr Protoc Cell Biol 2010;Chapter 18:Unit 18 10 11-13.

24. Stokman G, Qin Y, Genieser HG, Schwede F, de Heer E, Bos JL, Bajema IM, et al. Epac-Rap signaling reduces cellular stress and ischemia-induced kidney failure. Journal of the American Society of Nephrology : JASN 2011;22:859-872.

25. de Graauw M, Tijdens I, Cramer R, Corless S, Timms JF, van de Water B. Heat shock protein 27 is the major differentially phosphorylated protein involved in renal epithelial cellular stress response and controls focal adhesion organization and apoptosis. The Journal of biological chemistry 2005;280:29885-29898.

26. Benjamini YaH, Y. Controlling the False Discovery Rate: A Practical and Powerful Approach to Multiple Testing. Journal of the Royal Statistical Society. Series B (Methodological) 1995;57:289-300.

27. Nakamichi K, Saiki M, Kitani H, Kuboyama Y, Morimoto K, Takayama-Ito M, Kurane I. Roles of NF-kappaB and MAPK signaling pathways in morphological and cytoskeletal responses of microglia to double-stranded RNA. Neuroscience letters 2007;414:222-227.

28. Hoffmann A, Baltimore D. Circuitry of nuclear factor kappaB signaling. Immunol Rev 2006;210:171-186.

29. Guerin S, Baron ML, Valero R, Herrant M, Auberger P, Naquet P. RelB reduces thymocyte apoptosis and regulates terminal thymocyte maturation. Eur J Immunol 2002;32:1-9.

30. Mineva ND, Rothstein TL, Meyers JA, Lerner A, Sonenshein GE. CD40 ligand-mediated activation of the de novo RelB NF-kappaB synthesis pathway in transformed B cells promotes rescue from apoptosis. The Journal of biological chemistry 2007;282:17475-17485.

31. Wang X, Belguise K, Kersual N, Kirsch KH, Mineva ND, Galtier F, Chalbos D, et al. Oestrogen signalling inhibits invasive phenotype by repressing RelB and its target BCL2. Nature cell biology 2007;9:470-478.

32. Jacque E, Tchenio T, Piton G, Romeo PH, Baud V. RelA repression of RelB activity induces selective gene activation downstream of TNF receptors. Proc Natl Acad Sci U S A 2005;102:14635-14640.

33. Shain KH, Jove R, Olashaw NE. Constitutive RelB activation in v-Src-transformed fibroblasts: requirement for IkappaB degradation. J Cell Biochem 1999;73:237-247.

34. Kawai N, Tsuji S, Tsujii M, Ito T, Yasumaru M, Kakiuchi Y, Kimura A, et al. Tumor necrosis factor alpha stimulates invasion of Src-activated intestinal cells. Gastroenterology 2002;122:331-339.

35. Arthur WT, Ellerbroek SM, Der CJ, Burridge K, Wennerberg K. XPLN, a guanine nucleotide exchange factor for RhoA and RhoB, but not RhoC. The Journal of biological chemistry 2002;277:42964-42972.

36. Watanabe G, Saito Y, Madaule P, Ishizaki T, Fujisawa K, Morii N, Mukai H, et al. Protein kinase N (PKN) and PKN-related protein rhophilin as targets of small GTPase Rho. Science 1996;271:645-648.

37. Peck JW, Oberst M, Bouker KB, Bowden E, Burbelo PD. The RhoA-binding protein, rhophilin-2, regulates actin cytoskeleton organization. The Journal of biological chemistry 2002;277:43924-43932.

38. Igishi T, Mikami M, Murakami K, Matsumoto S, Shigeoka Y, Nakanishi H, Yasuda K, et al. Enhancement of cisplatin-induced cytotoxicity by ROCK inhibitor through suppression of focal adhesion kinase-independent mechanism in lung carcinoma cells. Int J Oncol 2003;23:1079-1085.

39. Song H, Gao D. Fasudil, a Rho-associated protein kinase inhibitor, attenuates retinal ischemia and reperfusion injury in rats. International journal of molecular medicine 2011;28:193-198.

40. Amano M, Nakayama M, Kaibuchi K. Rho-kinase/ROCK: A key regulator of the cytoskeleton and cell polarity. Cytoskeleton 2010;67:545-554.

41. Liu Y. Epithelial to mesenchymal transition in renal fibrogenesis: pathologic significance, molecular mechanism, and therapeutic intervention. Journal of the American Society of Nephrology : JASN 2004;15:1-12.

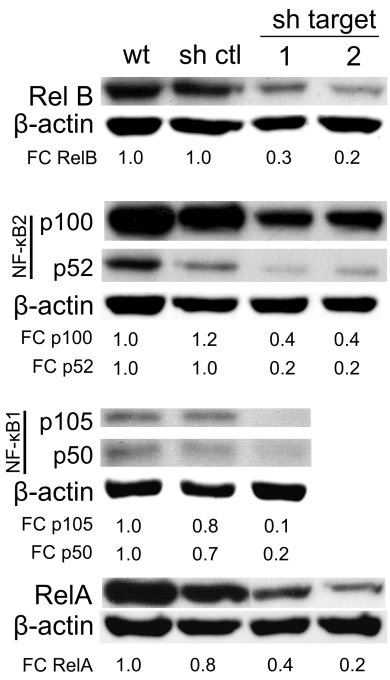
42. Liu Y. New insights into epithelial-mesenchymal transition in kidney fibrosis. Journal of the

American Society of Nephrology : JASN 2010;21:212-222.

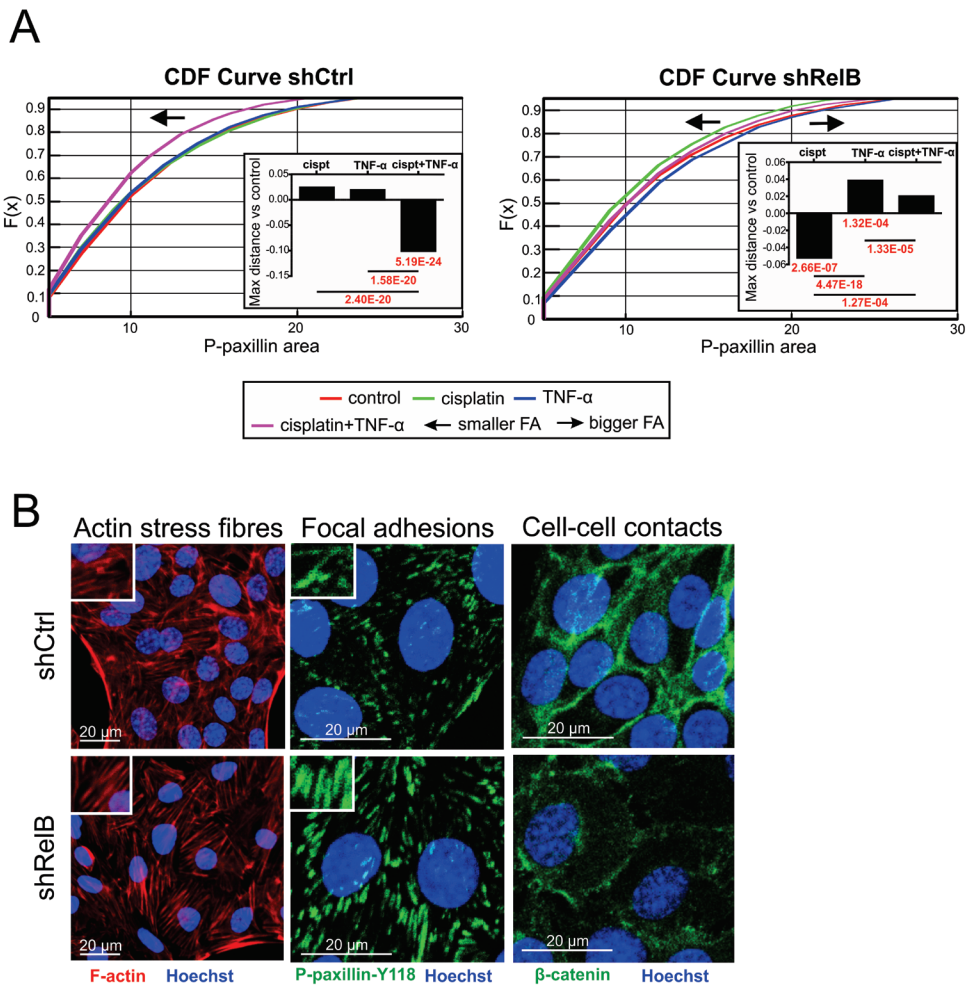
43. Hanner F, Sorensen CM, Holstein-Rathlou NH, Peti-Peterdi J. Connexins and the kidney. American journal of physiology. Regulatory, integrative and comparative physiology 2010;298:R1143-1155.

44. Zhang Y, Zhang X, Li L, Sun Y, Sun J. Apoptosis Progression in the Hair Cells in the Organ of Corti of GJB2 Conditional Knockout Mice. Clinical and experimental otorhinolaryngology 2012;5:132-138.

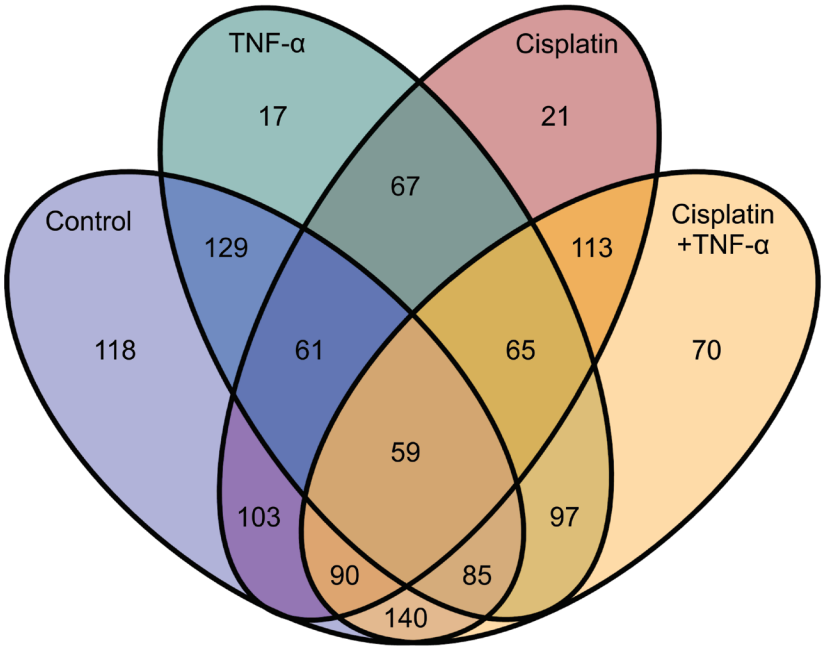
Supporting data



Supplemental Figure 1. Knock-down efficiency of the NF-κB members. The knock-down efficiency of the different NF-κB members was assessed by Western blotting. B-actin was used as a loading control and the quantification indicated is the mean of three independent experiments.



Supplemental Figure 2. Focal adhesion quantification of shCtrl and shRelB cells and morphology of the cells with TNF-α treatment alone. shCtrl and shRelB cells were exposed to cisplatin (20 µM) and/or TNF-α (8 ng/ml) for 8 hours and the effect of RelB knock-down on focal adhesions was assessed by staining of P-paxillin-Y118 followed by quantification as described under Fig. 1 and material and methods (A). After exposure of shCtrl and shRelB cells to TNF-α (8 ng/ml) for 8 hours, immuno-staining was performed to visualize the actin cytoskeleton, focal adhesions and cell-cell adhesions (B). The data are representative of three independent experiments.



Supplemental Figure 3. Comparison of the differentially expressed genes between treatments. The differentially expressed genes common for both shRelB#1 and #2 cell lines compared to wt+shCtrl cells with fold-change ≥1.5 or ≤-1.5 and FDR≤ 0.1 are represented for each treatment in a Venn diagram.

Supplemental Table 1. Differentially expressed genes common to both shRelB#1 and #2 cells compared to wt+shCtrl cells with FC≥ 1.5 or ≤ -1.5 and FDR≥ 0.1. The unique genes for each treatment are indicated in different sections.

Symbol	FC shRelB#1	FDR shRelB#1	FC shRelB#2	FDR shRelB#2
	unique genes for vehicle treatment			
1110067D22Rik	-1.960784314	0.0203	-1.7857143	0.0229
1500015O10Rik	-1.785714286	0.0153	-2	0.015
2210020M01Rik	-2.127659574	0.0255	-2.4390244	0.0229
9130017K11Rik	1.57	0.0105	1.57	0.0143
9930012K11Rik	-1.694915254	0.00704	-1.5625	0.0154
Actb	1.59	0.0324	2.08	0.00201
Adal	-1.612903226	0.0141	-1.5873016	0.0229
Adcy7	-2	0.00725	-2.3809524	0.0051
AI317395	-1.923076923	0.00121	-1.5873016	0.0203
Ampd3	-1.694915254	0.0231	-1.6129032	0.0131
Apol6	-1.5625	0.0277	-1.5384615	0.026
Arc	-2.272727273	0.000483	-1.6393443	0.00205
Arg2	3.13	0.00689	4.29	0.00257

Symbol	FC shRelB#1	FDR shRelB#1	FC shRelB#2	FDR shRelB#2
Arhgap18	-1.612903226	0.00968	-1.6949153	0.0132
Arhgap31	1.57	0.0166	1.8	0.00484
Arhgdib	-2	0.00341	-1.5625	0.0374
Atp9a	1.61	0.0192	1.63	0.00642
AU040829	1.69	0.00652	1.87	0.0103
B3galt1	-2.5	0.0183	-1.6666667	0.00108
Bend5	2.6	0.0582	2.34	0.0857
Blnk	-2	0.000676	-1.6666667	0.00577
Btbd19	-1.666666667	0.00428	-1.754386	0.0101
C1qtnf6	-1.923076923	0.0243	-1.9607843	0.0232
Cacna1a	-2.127659574	0.00452	-2.3255814	0.00266
Cacng8	1.89	0.00452	1.91	0.00295
Cbr2	-2.040816327	0.000238	-1.5873016	0.00291
Ccl7	2.34	0.000483	-1.8181818	0.00956
Cela1	-1.515151515	0.0152	-1.5151515	0.0105
Chst1	1.91	0.00256	1.82	0.0033
Cib2	-1.886792453	0.000356	-1.5384615	0.00412
Cmtm8	2.96	0.0000966	2.16	0.00383
Cp	2.12	0.00452	1.67	0.00614
Dbp	-1.818181818	0.00171	-1.8181818	0.000633
Dgat2	-1.639344262	0.00452	-1.5384615	0.00412
Dmd	-1.960784314	0.000133	-1.5873016	0.00192
Dopey2	1.69	0.0225	1.66	0.0192
E030010A14Rik	1.6	0.0586	2.07	0.0082
Ecscr	-1.612903226	0.0212	-1.9230769	0.0274
Efhd1	-1.960784314	0.000797	-2.0408163	0.000313
Emb	1.64	0.0873	2.46	0.00611
Erc2	-4.347826087	< 1e-07	-1.7857143	0.00236
Fam167a	-2.380952381	0.00239	-1.8518519	0.018
Fam46a	-2.083333333	0.00405	-2.1276596	0.00407
Galm	1.8	0.000622	1.62	0.00297
Gm22	-1.886792453	0.00166	-1.754386	0.00297
Gm5617	-1.587301587	0.0141	-1.6666667	0.00261
Gpr123	1.77	0.00337	1.65	0.00612
Gpr153	-1.724137931	0.0125	-1.5151515	0.00675
Hagh	-1.587301587	0.00165	-1.5625	0.00538
Hck	-1.960784314	0.00242	-1.754386	0.0101
Hs3st1	1.86	0.00122	1.57	0.0169
Id4	1.88	0.00501	1.57	0.032
Igfbp5	3.12	0.000476	3.87	0.000462
Il17re	-1.724137931	0.0202	-2.2222222	0.0021

Symbol	FC shRelB#1	FDR shRelB#1	FC shRelB#2	FDR shRelB#2
Il7	-1.886792453	0.000647	-1.7241379	0.00102
Itga9	1.58	0.00526	1.54	0.00795
Kctd15	-1.5625	0.0143	-2.1276596	0.000842
Kif13a	-1.538461538	0.00658	-1.5151515	0.0223
Kitl	-2.173913043	0.000133	-1.5384615	0.00291
Krt15	-3.225806452	0.00164	-1.9230769	0.0269
Lass2	1.71	0.00405	1.53	0.0206
Lcn2	1.81	0.0315	1.88	0.0276
Lifr	1.76	0.0138	3.32	0.000134
Lrrc8e	1.73	0.00456	1.69	0.00338
Lsr	2.09	0.00915	1.66	0.0648
Mcl1	1.62	0.00152	1.5	0.0033
Mgat4a	2.06	0.00145	2.76	0.000614
Mgat5	-1.612903226	0.00242	-1.6949153	0.00134
Mtmr11	1.64	0.000848	1.66	0.000736
Nid2	1.96	0.012	4.7	0.0000966
Npnt	1.53	0.0176	1.84	0.00962
Ociad2	1.5	0.0406	1.82	0.00169
Osmr	1.5	0.0129	1.51	0.00847
Pcdh18	-2.222222222	0.000622	-1.5384615	0.0791
Pcdh19	-2	0.00112	-1.754386	0.0118
Pde3b	3.22	0.00189	5.68	0.000201
Pde8a	2.44	0.0121	2.16	0.0267
Pdp1	-1.666666667	0.00361	-2	0.000555
Per2	-1.724137931	0.00685	-1.5384615	0.0406
Per3	-1.515151515	0.00501	-1.6129032	0.00188
Pla2g5	-1.818181818	0.0106	-1.8518519	0.00807
Plekha8	-1.639344262	0.00804	-1.6393443	0.000886
Plxna2	-1.538461538	0.00512	-1.5151515	0.0228
Pros1	1.59	0.00613	1.65	0.00324
Ptgs2	2.24	0.000716	1.88	0.00731
Rab2b	-1.5625	0.0233	-1.6393443	0.0173
Rgn	-1.818181818	0.000542	-1.5384615	0.00295
Rps6ka5	-1.666666667	0.0176	-1.8867925	0.00456
Rsad2	1.51	0.0369	-1.9230769	0.00297
S100g	-2.272727273	0.000459	-1.6129032	0.00538
Sema3a	-3.03030303	0.000603	-1.6949153	0.0158
Sema4a	-1.5625	0.00266	-1.6949153	0.000687
Sesn1	-1.639344262	0.0281	-1.5384615	0.00332
Sh3bp5	-1.754385965	0.0541	-1.6666667	0.0851
Sh3rf2	-1.818181818	0.0334	-1.7241379	0.0273

Symbol	FC shRelB#1	FDR shRelB#1	FC shRelB#2	FDR shRelB#2
Slc24a3	-2	0.000716	-1.7241379	0.00188
Slc4a11	1.61	0.0197	1.5	0.0388
Slc5a2	-1.851851852	0.0029	-1.6666667	0.0114
Slurp1	-2.380952381	0.000529	-2.1276596	0.00321
Spint1	1.98	0.0194	1.99	0.0307
Spn	-1.612903226	0.0337	-1.6129032	0.0346
St3gal4	-1.5625	0.00447	-1.6393443	0.00128
St8sia1	2.22	0.00264	1.57	0.0316
Stau2	1.6	0.0357	1.87	0.00907
Sv2a	2.11	0.000218	1.64	0.00538
Swap70	-1.923076923	0.0000966	-2.0833333	< 1e-07
Tert	-1.5625	0.0102	-1.6393443	0.00201
Tmem178	2.44	0.000306	4.31	< 1e-07
Tmem37	-1.851851852	0.000478	-1.8181818	0.000813
Tnfaip6	1.56	0.0199	1.73	0.0124
Tspan12	1.93	0.011	1.75	0.0263
Ttc7b	-1.587301587	0.0314	-1.8181818	0.00429
Uap1l1	-1.587301587	0.011	-1.5151515	0.0073
Vcan	-1.923076923	0.00721	-1.9230769	0.0205
Vegfc	2.15	0.0053	7.73	0.000291
Vgf	1.65	0.0172	1.51	0.0514
Zfp536	2.06	0.0469	1.66	0.0271
Zfp799	-2.380952381	0.0000595	-2.5	0.0000562
unique genes for TNF-α treatment				
4930402H24Rik	1.544065805	0.0493	1.62031597	0.0881
Adamts9	2.136414882	0.0571	1.64524615	0.0746
Arid1b	1.514541876	0.0841	1.7864859	0.0416
Ccl9	-4.201431493	0.0332	-3.9585742	0.0218
Chac1	-1.727069536	0.0844	-1.8541593	0.0834
Cx3cl1	-1.897849661	0.0219	-1.7845758	0.0371
Fam171a1	1.740714286	0.0481	2.03857143	0.0468
Insig1	-1.606590656	0.0433	-2.0153363	0.0304
Mcam	1.5728034	0.0413	1.8167729	0.0349
Mvd	-1.641079199	0.0381	-1.5742194	0.0698
Pdxk	-1.861617578	0.0481	-1.5031016	0.0951
Ppm1l	1.716269841	0.0485	1.92800454	0.0892
Rapgef5	1.85225421	0.0251	2.07224335	0.0951
Slc4a4	1.596525945	0.0725	1.52728864	0.0951
Sspn	-1.81003672	0.0365	-1.7964043	0.0881
Tanc2	1.949429846	0.0635	1.59940506	0.0615
Tmem71	-1.747893258	0.0304	-1.8644195	0.0372

Symbol	FC shRelB#1	FDR shRelB#1	FC shRelB#2	FDR shRelB#2
unique genes for cisplatin treatment				
Angptl4	-2.325581395	0.0547	-1.5151515	0.044
Apobec1	-1.639344262	0.0891	-1.5151515	0.0163
Arap2	1.76	0.0648	1.64	0.00817
Cdc42bpg	1.96	0.0539	1.58	0.0165
Celsr2	1.7	0.0366	1.61	0.0164
Csf1	1.53	0.0704	1.66	0.00555
Gm14137	-1.639344262	0.0324	-1.6393443	0.00502
Grb10	1.54	0.082	1.58	0.0118
Il15ra	-1.515151515	0.0846	-1.5384615	0.0343
Klf7	1.75	0.0498	1.57	0.0185
Klhl23	2.23	0.087	1.79	0.0689
Layn	-1.639344262	0.0574	-1.5384615	0.0138
Maf	-1.785714286	0.0811	-1.8867925	0.0138
Map3k6	-1.785714286	0.0704	-1.8181818	0.00595
Ndrg4	1.68	0.0844	1.68	0.00638
Nkain1	1.71	0.0571	1.54	0.0155
Nrip2	-1.724137931	0.0565	-1.5384615	0.0247
Pltp	-1.724137931	0.00412	-1.7241379	0.00181
Polr3gl	1.6	0.0328	1.6	0.00469
Rgs3	-1.515151515	0.0682	-1.6666667	0.00765
Suclg2	-1.538461538	0.0672	-1.5151515	0.039
unique genes for cisplatin+TNF-α treatment				
A930005H10Rik	-1.515151515	0.0114	-1.6393443	0.00548
Adh7	-1.724137931	0.00123	-1.5625	0.00196
AI414108	1.89	0.000893	1.6	0.00481
Ak3	-1.818181818	0.00116	-1.8181818	0.011
Ank3	-1.785714286	0.0086	-1.5384615	0.00428
Arhgef3	2.07	0.000137	1.68	0.00235
Aspg	-1.587301587	0.0159	-1.5625	0.0191
Camk2d	-1.886792453	0.00392	-1.6666667	0.00185
Car5b	-1.851851852	0.00117	-1.9230769	0.000717
Casp1	-1.886792453	0.00421	-1.5384615	0.0404
Casp12	-1.515151515	0.017	-1.5151515	0.0221
Cd83	2.46	0.00107	5.05	0.00328
Cldn1	-2.083333333	0.0000836	-1.5625	0.00252
Col4a1	2.2	0.0293	3.75	0.00467
Col4a2	2.29	0.0077	5.46	0.000107
Col4a5	-2.083333333	0.00158	-1.6666667	0.0495
Col6a2	-1.538461538	0.0371	-1.7241379	0.0103
Cstf3	1.7	0.00638	1.56	0.03

Symbol	FC shRelB#1	FDR shRelB#1	FC shRelB#2	FDR shRelB#2
Ctsh	3.55	0.000963	2.28	0.0509
Cyp39a1	-2.127659574	0.00291	-1.6393443	0.0225
Cyp3a13	-2.127659574	0.000855	-2.0408163	0.000912
Dennd2c	1.72	0.000855	1.6	0.00366
Elovl4	1.94	0.00282	1.83	0.00257
Ephb3	1.51	0.00126	1.53	0.0336
Fam84b	2.58	0.0624	3.04	0.0651
Fbln2	-1.5625	0.0086	-1.7241379	0.00491
Frk	-1.612903226	0.021	-2	0.0162
Frmd4b	-2.222222222	0.000525	-1.6949153	0.00457
Fubp1	1.64	0.0094	1.58	0.0622
Gbe1	-1.724137931	0.0113	-1.5384615	0.00491
Gjb2	3.9	0.0201	4.09	0.000238
Hey2	1.67	0.0154	1.77	0.0111
Hsd17b11	-1.538461538	0.0182	-1.6393443	0.00435
Il1rn	-2.702702703	0.000515	-1.7857143	0.00509
Kcnq1ot1	1.65	0.00644	1.8	0.00632
Krt12	-1.754385965	0.03	-2.0408163	0.0421
Lcorl	1.6	0.003	1.51	0.0683
Leprel1	-2.040816327	0.00443	-1.6393443	0.00695
Loxl3	-1.639344262	0.00479	-2.173913	0.000442
Lrp2	-1.923076923	0.0213	-2	0.0272
Luc7l2	1.99	0.00835	1.67	0.0145
Mgst2	-1.724137931	0.00176	-1.6949153	0.00404
Mme	-2.127659574	0.00107	-1.5151515	0.0542
Myo6	-1.5625	0.00555	-1.5873016	0.0032
Nipal1	1.78	0.0209	1.64	0.0427
Nt5c2	-1.818181818	0.00866	-1.5384615	0.0213
Oxct1	-1.785714286	0.00737	-1.7857143	0.0118
Pcca	-2.127659574	0.000712	-1.6129032	0.034
Phkb	-2	0.00993	-2.0833333	0.000814
Psrc1	1.87	0.00399	1.72	0.0262
Ptp4a3	1.68	0.0868	2.28	0.0156
Ptplad2	-2.127659574	0.00799	-1.8518519	0.00676
Rab14	1.61	0.0178	1.52	0.038
Rap1a	1.51	0.00779	1.55	0.00722
Rhpn1	1.83	0.00161	1.76	0.00937
Sec14l2	1.72	0.0661	1.86	0.0261
Sema3c	-2.702702703	0.000289	-1.5151515	0.00491
Slc22a4	-1.694915254	0.00178	-1.6666667	0.00147
Spib	-2.040816327	0.0301	-2.0833333	0.0919

Symbol	FC shRelB#1	FDR shRelB#1	FC shRelB#2	FDR shRelB#2
Sprr1a	-3.125	0.0000836	-2.5	0.000107
Stbd1	2.76	0.0254	2.63	0.0566
Tmtc3	1.57	0.0124	1.59	0.0257
Trim2	-1.587301587	0.00294	-1.5151515	0.00616
Trp53i11	1.65	0.00542	1.71	0.0116
Trpc1	1.85	0.00201	1.59	0.0205
Ttc9	1.99	0.00195	2.17	0.0229
Ubd	-1.587301587	0.0669	-1.754386	0.0742
Ubxn2b	1.54	0.0183	1.52	0.0114
Zfp37	1.96	0.000855	2.02	0.000912
Zfr	1.76	0.017	1.64	0.0706
common genes between the different treatments				
0610040B09Rik	-2.631578947	0.0000595	-1.6666667	0.00906
1110012J17Rik	1.78	0.0254	1.96	0.00313
1600021P15Rik	2.12	0.0126	2.38	0.00585
1700012D01Rik	-1.515151515	0.00729	-1.5384615	0.0423
1700016C15Rik	-2.380952381	0.000133	-2	0.000614
2010107G23Rik	2.42	0.000377	1.97	0.00351
4833427G06Rik	-1.694915254	0.00157	-1.8518519	0.000478
4930423D22Rik	1.87	0.0115	1.58	0.0719
5330426P16Rik	1.69	0.00714	1.89	0.00202
5730433N10Rik	1.68	0.0736	1.75	0.0589
8030494B02Rik	1.72	0.00067	1.72	0.0169
A230061C15Rik	2.41	0.000684	1.52	0.0307
Ablim1	-2.173913043	0.0363	-1.8181818	0.00765
Acsm2	-4.166666667	0.00121	-2.173913	0.0351
Add3	2.34	0.00671	2.39	0.00141
AI467606	-4.166666667	0.000519	-4.7619048	0.000394
Aif1l	-1.538461538	0.0108	-2.4390244	0.000134
Akr1c12	-2.325581395	0.0000595	-1.8518519	0.000641
Akr1c13	-1.5625	0.00132	-1.6949153	0.000511
Alcam	-1.923076923	0.00281	4.03	< 1e-07
Amigo2	-2.083333333	0.0426	-1.8867925	0.00143
Angpt4	-3.571428571	0.00266	-1.9230769	0.00373
Ankrd29	-2.43902439	0.000238	-1.6666667	0.00113
Ankrd34b	2.04	0.0677	1.67	0.0102
Antxr1	-5.555555556	< 1e-07	-7.1428571	< 1e-07
Aph1a	1.7	0.000542	1.6	0.00236
Aqp5	-4.761904762	0.0000595	-5.8823529	< 1e-07
Arnt	1.54	0.00205	1.87	0.000235
Arrdc4	1.77	0.1	2.18	0.00649

Symbol	FC shRelB#1	FDR shRelB#1	FC shRelB#2	FDR shRelB#2
Ascl2	1.95	0.0697	1.61	0.0134
Aspa	-5.555555556	< 1e-07	-2.8571429	0.0000966
Atp10d	2.04	0.00802	5.01	< 1e-07
Atp8a1	3.65	< 1e-07	2.56	0.00126
AU021092	-2.702702703	0.000191	-2.173913	0.00068
AW552393	1.73	0.00151	1.77	0.0144
B4galt4	2.18	0.0125	2.02	0.0363
Baiap2l1	3.92	0.0000966	3.62	0.0000966
BB287469 /// Eif1a /// Gm2016 /// Gm2022 ///				
Gm2035 /// Gm4027 /// Gm5039 /// Gm5662	-2.857142857	0.0177	-3.030303	0.0169
BC037703	1.6	0.00779	1.65	0.0706
BC066028	-1.923076923	0.00294	-1.8867925	0.00356
Bckdhb	-2.127659574	0.0704	-2.173913	0.00408
Bhlhb9	2.67	0.00827	2.01	0.0444
Bmp4	-1.639344262	0.00116	-1.9230769	0.000497
C130026I21Rik ///				
LOC100041885	-2.083333333	0.0494	-3.125	0.00654
C77370	1.96	0.00483	2.65	0.00142
Cachd1	1.91	0.0053	3.02	< 1e-07
Calml4	-2.272727273	0.000218	-1.6666667	0.00112
Capg	-1.960784314	0.0185	-2.7027027	0.00962
Capn1	-1.851851852	0.099	-1.6949153	0.0296
Car12	-2.857142857	< 1e-07	-2.4390244	0.0000562
Ccl17	-2.857142857	0.000163	-3.030303	0.000742
Ccnd2	-4.545454545	0.0000595	-3.030303	< 1e-07
Cd40	2.17	0.000666	2.27	0.000291
Cdc42se1	1.62	0.00119	1.72	0.000655
Cdh11	1.81	0.0406	1.75	0.0531
Celsr1	2.57	0.000622	2.73	0.000412
Cgn	2.2	0.000218	2.07	0.0000966
Chic1	2.03	0.00605	2.61	0.00143
Ckap4	1.62	0.0353	1.59	0.0229
Clgn	1.79	0.00119	2.67	0.0000562
Clmn	1.55	0.0937	1.8	0.0257
Cnn1	3.257714286	0.00817	1.62457143	0.0599
Col4a1	2.59	0.0551	4.36	0.000172
Col4a2	2.48	0.0386	6.63	0.000668
Cox7a1	-1.612903226	0.00381	-1.5384615	0.0215
Crip1	-1.515151515	0.00889	-1.754386	0.00108

Symbol	FC shRelB#1	FDR shRelB#1	FC shRelB#2	FDR shRelB#2
Crlf1	1.74	0.0542	1.56	0.0228
Cxcl14	2.37	0.00105	2.14	0.00135
Cxcr7	-1.995400157	0.0196	-1.6958211	0.0468
Cytip	-1.754385965	0.001	-1.5384615	0.0377
D0H4S114	3	0.021	8.36	< 1e-07
D15Wsu126e	2.08	0.00689	1.73	0.0192
D4Bwg0951e	-2.777777778	0.0000966	-2.0833333	0.000758
D630033O11Rik	-1.886792453	0.0205	-1.9230769	0.0212
D7Wsu130e	-1.818181818	0.0201	-1.5873016	0.0147
Dapk1	2.05	0.09	2.45	0.0342
Ddit4l	2.53	0.0185	2.5	0.0221
Dkk3	-2	0.0302	-1.6393443	0.00169
Dmxl2	-1.515151515	0.0108	-1.7241379	0.00134
Dsel	1.68	0.0208	2.03	0.00208
E330009J07Rik	1.92	0.0046	1.89	0.00183
Eno3	-1.886792453	0.0308	-3.125	0.00132
Enpep	1.98	0.0507	2.31	0.0218
Ensa	1.66	0.000622	1.52	0.00259
ENSMUSG00000068790 /// Gm10128 /// Gm2897 /// Gm3002 /// Gm3373 /// Gm3558 /// Gm3696 /// Gm8348	1.75	0.001	1.62	0.00189
Eppk1	2.45	0.00235	1.75	0.0229
Ereg	-2.777777778	< 1e-07	-3.125	0.0000562
Eya4	-2.5	0.0000595	-1.5384615	0.00965
Fam57a	1.65	0.00119	1.9	0.000201
Fam63a	2.05	0.000163	1.89	0.000201
Fam73a	1.88	0.0174	2.17	0.00843
Fcgr2b	-2	0.000133	-2.2727273	0.000412
Fgfr3	-3.448275862	0.000459	-2	0.0185
Figf	-2.5	< 1e-07	-3.2258065	< 1e-07
Fmod	-3.03030303	0.000925	-1.6949153	0.00297
Foxred2	-2.941176471	0.00026	-4.5454545	< 1e-07
Gabpb2	1.92	0.00215	2.41	0.0000562
Galnt12	2.86	0.00265	2.31	0.0112
Ggh	2.08	0.0212	2.4	0.00807
Gldc	3.52	0.00065	7.24	0.0000562
Gnai1	2.31	0.0507	4.42	0.00227
Golph3l	1.600819882	0.0519	1.63361517	0.0962
Gpc6	-1.666666667	0.0582	-3.2258065	0.000562

Symbol	FC shRelB#1	FDR shRelB#1	FC shRelB#2	FDR shRelB#2
Gpr137b /// Gpr137b-ps	-1.785714286	0.00373	-1.5625	0.0171
Gpr146	-1.666666667	0.0168	-1.5384615	0.00797
Gsta3	-5	< 1e-07	-1.7857143	0.000201
Gsta4	-1.533028571	0.0557	-1.7465009	0.0468
Gstm2	-2.773667645	0.0133	-1.7039724	0.0853
Gstm7	-1.666666667	0.0105	-1.5625	0.0332
Gzmd /// Gzme	1.87	0.00129	1.66	0.0239
H2-DMb2	-1.73388203	0.0351	-1.6898396	0.0534
Heatr7b1	-2.5	< 1e-07	-2	0.0000562
Hgfac	-1.886792453	0.000622	-1.8867925	0.000655
Hist1h1c	1.64	0.00128	2.15	0.0000966
Hist1h4a /// Hist1h4b ///				
Hist1h4f /// Hist1h4m	1.5	0.0726	1.51	0.0794
Hist2h2bb	1.98	0.00124	2.21	0.000347
Hist2h3c1	2.25	0.000445	2.47	0.000172
Hist2h3c2-ps	1.56	0.0353	1.8	0.00901
Hook1	2.17	0.0175	1.95	0.00771
Ica1	3.97	< 1e-07	3.1	0.0000966
Ifi44	3.36	< 1e-07	1.99	0.00265
Igsf3	2.43	0.001	2	0.000562
Il15ra	-1.515151515	0.0846	-1.5384615	0.0343
Il18	-1.515151515	0.0506	-1.5151515	0.00984
Insl6	-1.785714286	0.0136	-1.8867925	0.00956
Iqcg	-1.587301587	0.0266	-1.8181818	0.0106
Isoc1	2.66	0.0115	2.42	0.000375
Kcnj15	-1.694915254	0.00294	-1.8867925	0.003
Kcnn4	-1.754385965	0.0261	-1.6393443	0.044
Kctd1	-1.960784314	0.000163	-1.7241379	0.000583
LOC100503868	-2.5	0.000892	-1.9607843	0.00312
LOC100504029	1.753493014	0.0381	1.58848969	0.0931
LOC100504121	-1.587301587	0.0294	-1.6393443	0.0181
LOC100504883	1.907168038	0.0251	2.39130435	0.0949
Lonrf3	2.24	0.0678	1.84	0.00807
Lox	3.05	0.00613	2.2	0.0309
Lrrc8c	1.89	0.0621	1.67	0.0844
Ly6f	-2.5	0.00283	-2.0833333	0.00882
Lysmd2	2.44	0.0000966	2.12	0.000313
Maf	-1.785714286	0.0811	-1.8867925	0.0138
Marcks	1.521545473	0.0644	3.0375703	0.00817
Mfsd6	3.47	0.0166	2.22	0.000725
Mlf1	1.67	0.0713	4.8	0.000497

Symbol	FC shRelB#1	FDR shRelB#1	FC shRelB#2	FDR shRelB#2
Mllt11	1.87	0.000377	1.77	0.000562
Ms4a4d	-2.564102564	0.0056	-2.5641026	0.00802
Msln	-1.754385965	0.00483	-2.2727273	0.000641
Myh10	4.08	0.00378	4.43	0.00227
Ndn	3.81	0.0289	2.61	0.0203
Nipa1	1.91	0.00118	2.07	0.000971
Nmb	1.5	0.0764	2.15	0.00189
Nr1h4	-1.768838305	0.0493	-1.5733985	0.098
Ntn1	-1.960784314	0.0484	-1.8518519	0.00307
Nupr1	-1.612903226	0.00149	-1.754386	0.000347
Ogfrl1	1.96	0.0035	1.62	0.00428
Ogn	-9.090909091	< 1e-07	-1.9607843	0.00068
Olfm1	-2.702702703	0.000445	-3.125	0.000687
Otud7b	2.15	0.0000595	2.17	0.0000966
Panx1	1.59	0.0159	1.53	0.0125
Pard3b	2.84	0.002	3.21	0.00152
Pard6g	5.21	0.000459	5.02	0.000668
Pcdh17	-4.545454545	0.00135	-4.7619048	0.00128
Pcp4	2.92	0.0000595	2.33	0.0000562
Pde8a	1.997545582	0.0219	1.55358854	0.0917
Pdlim1	1.64	0.0347	1.66	0.0466
Pdlim2	-1.666666667	0.00294	-1.8518519	0.00287
Pdzrn3	3.36	< 1e-07	2.5	0.0000562
Peg3	8.59	0.0000966	13.23	< 1e-07
Pgcp	-1.960784314	0.00193	-1.5384615	0.0227
Pi4kb	1.97	0.00026	1.98	0.000594
Pip5k1a	1.59	0.00351	1.78	0.000959
Plscr4	-1.818181818	0.000711	-1.7241379	0.000478
Pmaip1	2.93	0.000622	2.71	0.00126
Pmp22	-1.886792453	0.0412	-1.5384615	0.012
Pogk	3.3	0.001	3.03	0.0055
Pogk /// Tada1	1.83	0.00841	1.93	0.00647
Pogz	2.11	0.000622	2.14	0.000134
Postn	-4.545454545	0.0000595	-2.0408163	0.0808
Ppp1r9a	1.92	0.00542	3.19	0.00238
Prickle1	4.33	< 1e-07	6.11	< 1e-07
Prkcdbp	-1.694915254	0.00678	-1.6393443	0.0181
Prkg2	-1.785714286	0.00214	-1.754386	0.0175
Prodh	-1.5625	0.0121	-2.6315789	0.000134
Prom1	2.47	0.0363	2.72	0.0243
Prpf3	1.7	0.000478	1.62	0.00108

Symbol	FC shRelB#1	FDR shRelB#1	FC shRelB#2	FDR shRelB#2
Prune	1.66	0.00235	1.59	0.00512
Psmd4	1.67	0.0012	1.55	0.00271
Ptgfrn	1.53	0.0113	1.68	0.00435
Ptpla	1.56	0.0165	2.17	0.000594
Ptpn18	2	0.00464	1.68	0.0347
Ptpre	-2.083333333	0.000478	-1.9230769	0.00102
Ptprg	-2.127659574	0.0406	-2.3809524	0.00685
Ramp3	2.92	0.000416	2.1	0.00412
Relb	-2.857142857	< 1e-07	-4.7619048	< 1e-07
Rfx5	1.66	0.000753	1.61	0.000813
Rgs10	-1.538461538	0.017	-2.1276596	0.00102
Rnf130	2.45	0.00418	2.34	0.00629
Rprd2	1.65	0.0156	1.63	0.000562
S100a4	-5.263157895	0.0000966	-6.25	0.000333
Scarb2	-1.724137931	0.001	-1.754386	0.00163
Scd1	-2.43902439	0.000334	-1.6949153	0.000394
Scel	-1.886792453	0.00146	-1.6393443	0.00793
Scnm1	1.59	0.00613	1.5	0.0123
Selm	-1.658939515	0.043	-1.7915258	0.0357
Serpinb6b	-2.702702703	0.0111	-1.6129032	0.00326
Serpinb9b	-1.666666667	0.0117	-2.0833333	0.00349
Serpine2	8.38	0.0106	8.45	0.0119
Setdb1	1.83	0.000238	1.74	0.000347
Sgcb	1.539942053	0.0677	1.5656043	0.0931
Slc15a2	-3.03030303	< 1e-07	-2.6315789	< 1e-07
Slc16a4	-1.587301587	0.024	-1.8181818	0.00888
Slc22a15	1.82	0.00156	2.05	0.00108
Slc40a1	1.53	0.00337	2.19	0.0000562
Slc43a2	-4.347826087	< 1e-07	-3.5714286	< 1e-07
Slc7a3	-4.761904762	< 1e-07	-3.7037037	< 1e-07
Snai2	2.65	0.00294	2.32	0.0106
Snrpd3	1.58	0.0249	1.62	0.01
Sp8	-2.631578947	0.0000595	-2.6315789	0.0000562
Speg	-1.587301587	0.0126	-1.5625	0.0193
Stag3	1.59	0.00266	1.86	0.00109
Stox2	2.96	0.0268	3.11	0.0173
Sult1a1	-2.857142857	< 1e-07	-2.9411765	< 1e-07
Sult1d1	-9.090909091	< 1e-07	-4.3478261	< 1e-07
Svip	1.63	0.0495	2.06	0.00675
Synm	1.77	0.000587	1.63	0.000742
Syt8	-3.571428571	0.00761	-2.9411765	0.0173

Symbol	FC shRelB#1	FDR shRelB#1	FC shRelB#2	FDR shRelB#2
Tars2	1.73	0.000981	1.6	0.00183
Tbc1d2b	1.81	0.0115	2.19	0.00276
Tbx20	-2.5	0.0000595	-1.7241379	0.0039
Tinag	-2.112130771	0.0143	1.55655126	0.0917
Tlr4	-1.515151515	0.00412	-1.5873016	0.00297
Tmem141	2.55	0.000334	2.01	0.000794
Tmem159	1.82	0.00452	1.98	0.00172
Tmie	-2.222222222	0.0000595	-1.8518519	0.000926
Tmlhe	-2.702702703	0.000191	-1.8518519	0.00353
Tmod4	2.15	0.000529	1.61	0.0169
Tnfaip2	-1.724137931	0.00451	-2	0.00281
Tnni2	-2	0.0901	-1.5873016	0.0378
Tpd52l1	2.23	0.00273	1.94	0.00538
Tram1l1	2.28	0.000191	5.93	< 1e-07
Tspan6	1.66	0.0213	1.93	0.0214
Tubb2a-ps2 /// Tubb2b	1.72	0.0836	-1.9230769	0.0482
Tuft1	2.09	0.0000966	2.19	0.0000562
Txnip	1.87	0.013	1.71	0.0131
Ugt1a1 /// Ugt1a10 /// Ugt1a2// Ugt1a5 /// Ugt1a6a /// Ugt1a6b /// Ugt1a7c /// Ugt1a9	-2.777777778	0.000238	-1.6949153	0.000511
Unc13b	2.79	0.0046	2.14	0.00807
Upk3b	-3.571428571	< 1e-07	-3.030303	< 1e-07
Vamp5	-1.960784314	0.00138	-1.7857143	0.00228
Vash1	1.53	0.00713	1.65	0.00712
Vgll3	-3.448275862	0.000653	-5.2631579	0.000235
Vps72	1.87	0.000555	1.83	0.000878
Zbtb10	1.85	0.00615	1.69	0.0224
Zfp612	2.27	0.00142	2.29	0.00435
Zfp687	1.68	0.00132	1.94	0.0000562
Zfp760	-1.822495606	0.0351	-2.0809365	0.0514